Final Technical Report (FTR) Instructions

Solar Energy Technologies Office (April 2020)

Purpose: To provide DOE with a concise technical review of the award's final outcomes including: technical impact, scholarship, and intellectual property. Include sufficient detail to assess the project's technical merit relative to the objectives, milestones, and go/no-go decision points. The final report should clearly articulate the accomplishments made during the award and the importance of the results. The report should be self-supporting; in other words, from reading the report alone, the accomplishments and value of the work completed should be apparent. The report is intended to demonstrate how your efforts have mitigated the technical risks and uncertainties associated with converging on the final milestones/deliverables.

Format: The FTR is modeled after a technical manuscript for a peer-reviewed publication. The report is expected to be 20-50 pages using 1-inch margins, single spacing, and Arial size 12 font, with the following file name convention: last 4 (non-lab) or 5 (lab) digits of the award number, "FTR", and recipient name. Reports must be submitted electronically in non-protected Adobe Portable Document Format (PDF).

Where to File: All FTRs should be uploaded to: www.osti.gov/elink-2413. Non-lab FTRs should also be uploaded to: https://www.eere-pmc.energy.gov/SubmitReports.aspx, while national laboratory FTR's should be emailed to the respective technology manager and project officer, with a copy sent to the subprogram email box if so directed (e.g. cspsolar@ee.doe.gov, sisolar@ee.doe.gov).

When to File: The Federal Assistance Reporting Checklist (FARC) that came with your award package contains specific instructions regarding when to file depending on which subprogram your project is associated (*See: "EERE Special Instructions" on page 2*).

Protected Data: The FARC also outlines what to do if your FTR contains protected data (*See: "EERE Special Instructions" on page 2 and Section II.A on page 21*). With the pace of solar technology advancement, it is in the best interest of all parties to have a version of your report available to public while the information is still relevant.

Final Technical Report (FTR) Template

Agency/Office/Program	DOE/EERE/Solar Energy Technology Office	
Award Number	DE-EE0008543	
Project Title	Comparative Life Cycle Analysis of Scalable Single-Junction and Tandem Perovskite Solar Cell (PSC) Systems	
Principal Investigator	Vasilis Fthenakis, Senior Research Scientist Email: vmf5@columbia.edu Phone: 631-618-1717	
Business Contact	Name, Title, Email, Phone	
Submission Date	Jessy George Sponsored Project Administrator jg3721@columbia.edu 212-854-0372	
DUNS Number	049179401	
Recipient Organization	Columbia University Company	
Project Period	**Start:** 03/01/2019	**End:** 07/31/2020
Project Budget	Total $251,950 (DOE: $199,911; C/S: $52039)	
Submitting Official Signature	*Vasilis Fthenakis*	

1. **Acknowledgement:** "This material is based upon work supported by the U.S. Department of Energy's Office of Energy Efficiency and Renewable Energy (DOE-EERE) under the Solar Energy Technologies Office (SETO) Award Number DE00008453".

2. **Disclaimer**: "This report was prepared as an account of work sponsored by an agency of the United States Government. Neither the United States Government nor any agency thereof, nor any of their employees, makes any warranty, express or implied, or assumes any legal liability or responsibility for the accuracy, completeness, or usefulness of any information, apparatus, product, or process disclosed, or represents that its use would not infringe privately owned rights. Reference herein to any specific commercial product, process, or service by trade name, trademark, manufacturer, or otherwise does not necessarily constitute or imply its endorsement, recommendation, or favoring by the United States Government or any agency thereof. The views and opinions of authors expressed herein do not necessarily state or reflect those of the United States Government or any agency thereof."

3. Executive Summary:

Efficient, low-cost solar cells based upon perovskites have the potential to transform the US and global energy portfolio and improve energy security if they can be manufactured in an environmentally sustainable manner. However, previous life cycle analyses (LCA) of perovskite solar cells (PSC) used lab recipes to project the environmental impact of industrial PSC production – using materials and processes that may not be representative of industrial productions due to high material waste and complex synthesis – and such studies were limited to a few single-junction technologies. Thus, the goal of this project was threefold: a) to review the most promising for industrial production single-junction and tandem PSC technologies, b) to build life-cycle materials inventories that reflect scalable production of these technologies, and c) to conduct comprehensive life-cycle analysis of these technologies and compare their environmental impact with those of established commercial technologies.

In response, this project identified challenges for fabrication transitioning from laboratory to sustainable industrial production, developed life-cycle inventory (LCI) data for scaling to industrial production four promising single-junction and three tandem PSC systems and produced life-cycle-investigations using, as metrics, a complete spectrum of energy, environmental and ecological impact indicators. Special focus was given to the use of lead, silver and indium in PSC.

The project used the Life Cycle Assessment (LCA) methodology as standardized by the Society of Environmental Toxicology and Chemistry (SETAC), ISO standards 14040 and 14044, and the International Energy Agency PVPS Task 12 LCA guidelines. LCA allows the calculation of a number of energy and environmental and impact categories, including energy cumulative energy demand (CED), global warming potential (GWP), human toxicity potential (HTP), eco-toxicity potential (ETP), abiotic resource depletion potential (ADP), acidification potential (AP), ozone depletion potential (ODP), photochemical oxidation potential (POP), eutrophication potential (EP). In addition to those, we calculated the Energy Pay-Back Time (EPBT) and the Energy Return On Investment (EROI). We provide LCA impacts for complete perovskite PV systems – including balance of system components – installed at three irradiation levels and considering reference and future potential module efficiencies. Finally, a sensitivity analysis on perovskite lifetime has been performed, considering 10, 20 and 30 years.

Contribution analysis of the impacts of each material and layer of PSC shows, that the use of Pb in metalorganic PSC does not result in significant environmental impacts as the major contributions to environmental indicators arise from the use of Ag and encapsulation materials. Solution-based PSC manufacturing was found to be less impactful to the environment than vapor-based fabrication, and roll-to-roll (RtR) printing uses less energy and generates the lowest emissions. PSC produced with RtR manufacturing could reach the same Energy Return on Energy Investment (EROI) as that of crystalline-Si PV within 12 years of life, whereas the most energy demanding spray coating on rigid substrates, would require a 20-yr life to match the EROI of 30-yr lasting silicon PV. This work lays the foundation for sustainability investigations in a comparative context of large-scale production and deployment of PSC. The results of this project have the potential to have a significant impact on the future of PV manufacturing, by providing industry, policy-makers, and academia with insights necessary to choose which, if any, lead-based solar cell life cycles are environmentally sustainable.

4. Table of Contents:

5. Background:

As highlighted by a team of NREL researchers [1], the early perovskite life cycle analysis (LCA) literature was limited to examining a few of the several promising technologies and did not offer comprehensive comparison with existing PV technologies. Also, life-cycle studies of PSC were based on linear extrapolations of laboratory data, assuming materials and processes that may not be representative of industrial productions due to high material waste and complex synthesis – such as Spiro-MeoTAD and spin coating [2-12]. In addition to this, previous LCA studies gave widely different results.
In this project we started with critically reviewing the PSC LCA literature, explained the reasoning for a wide divergence of results, and determined which data apply to scalable industrial production, materials and processes. We used the LCA methodology as standardized by the Society of Environmental Toxicology and Chemistry (SETAC), ISO standards 14040 and 14044, and the International Energy Agency PVPS Task 12 LCA guidelines [13-18].
Table 1 shows a summary of perovskite device stack architectures analyzed by previous LCA studies with materials and perovskite deposition processes for single-junction and tandem perovskite solar cells.

Table 1: LCA studies on single-junction and tandem perovskite solar cells with architecture type, material configurations and deposition processes.

Architecture	**Material Configuration**	**Perovskite deposition process**	**Reference**
Single-junction	FTO/TiO_2/Pb-based perovskite/SpiroMeOTAD/Ag	thermal co-evaporation	Espinosa et al., 2015 [2]
	ITO/PEDOT:PSS/Pb-based perovskite/PCBM/Al	spin coating	
	ITO/PEDOT:PSS/Pb-based perovskite/PCBM/Al	spin coating	Serrano-Lujan et al., 2015 [3]
	FTO/TiO_2/Pb-based perovskite/Spiro-OMeTAD/Ag	thermal co-evaporation	
	FTO/TiO_2/tin-based perovskite+TiO2/ Spiro-OMeTAD/Au	spin coating	
	FTO/TiO_2/Pb-based perovskite/ Spiro-MeOTAD/Au	spin coating	Gong et al., 2015 [4]
	ITO/ZnO/Pb-based perovskite/P3HT/Ag	spin coating	

	FTO/SnO_2/Pb-based perovskite/CuSCN/MoO_x-Al	thermal co-evaporation	Celik et al., 2016 [19]
	FTO/SnO_2/Pb-based perovskite/CuSCN/MoO_x-Al	spray coating	
	FTO/SnO_2/Pb-based perovskite/C-paste	spray coating	
	FTO/TiO_2/m-TiO_2/$MAPbI_3$/Spiro-OMeTAD/Au	vapour deposition	Ibn-Mohammed et al., 2017 [8]
	FTO/TiO_2/m-TiO_2/CsFAPbIBr/CuSCN/Cu	spin coating	
	FTO/TiO_2/Pb-based perovskite /electrolyte/Pt	spin coating	Zhang et al., 2015 [12]
	FTO/TiO_2/TiO_2paste/$MASnI_{3-x}Br_x$/Spiro-OMeTAD/Au	spin coating	Zhang et al., 2017 [9]
	FTO/TiO_2/TiO_2paste/$MAPbI_3$/Spiro-OMeTAD/Au	spin coating	
	FTO/TiO_2/$FAPbI_3$/Spiro-OMeTAD/Au	spin coating	
	FTO/TiO_2/TiO_2paste/$CsPbBr_3$/Spiro-OMeTAD/Au	spin coating	
	FTO/TiO_2/TiO_2paste/$MAPbI_2Cl$/Spiro-OMeTAD/Au	spin coating	
	FTO/TiO_2/$MAPbI_3$/Spiro-MeOTAD/Au	spin coating	Alberola-Borras et al., 2017 [10]
	FTO/TiO_2/Pb-based perovskite/Spiro-OMeTAD	spin coating	Sánchez et al., 2019 [11]
	FTO/TiO_2/Pb-based perovskite/ZrO_2/carbon	spin coating	Alberola-Borras et al., 2018 [7]
	FTO/SnO_2/$MAPbI_3$/MoOx-Al/C-paste	thermal co-evaporation	Billen et al., 2019 [21]
	FTO/SnO_2/$MAPbI_3$/CuSCN/MoOx-Al/C-paste	spray coating	
	ITO/SnO_2/Pb-based perovskite/NiOx/Ag	thermal evaporation of PbI_2 and slot-die coating of MAI	Itten and Stucki, 2017 [20]
2T Tandem: Si/PK_{Pb}	Ag/ITO/NiOx/Perovskite/SnO_2/n-μ-c-Si/p-μ-c-Si/i-a-Si/n-a-Si/ITO/Ag	thermal evaporation of PbI2 and slot-die coating of MAI	
	Ag/ITO/MoO_3/Spiro-OMeTAD/Perovskite/TiO_2/HIT Si/Ag	spin coating	Lunardi et al., 2017 [6]
	Au/ITO/MoO_3/Spiro-OMeTAD/Perovskite/TiO_2/HIT Si/Ag	spin coating	
	Al/ITO/ZnO/PCBM/Perovskite/PEDOT:SSS/ITO/Si (n)/Si (p)/Al	spin coating	

	Top Cell: Encap./ITO/MoO_3/SpiroOMeTAD/PK_{Pb}/PCBM; Tunnel: ZnO:In; Bottom Cell: i a-Si/p a-Si/Si/i a-Si/n a-Si/ITO/Ag	spin coating	Celik et al., 2017 [5]
2T Tandem: CIGS/PK_{Pb}	Top Cell: Encap./FTO/TiO_2/PK_{Pb}/Spiro-OMeTAD; Tunnel: MoO_3/ZnO/ ZnO:Al; Bottom Cell: CdS/CIGS/Mo/Glass	spin coating	
2T Tandem: CZTS/PK_{Pb}	Top Cell: Encap./Al/PCBM/PK_{Pb}/PEDOT:PSS; Tunnel: ITO Bottom Cell: CdS/CZTS/Mo/Glass	spin coating	
2T Tandem: PK_{Sn}/PK_{Pb}	Top Cell: Glass/ITO/NiO/PK_{Pb}/PCBM Tunnel: ITO Bottom Cell: PEDOT:PSS/ $PK_{Sn,Pb}$/ PCBM/Ag/Encap.	spin coating	
Only perovskite layer	$MAPbI_3$	spin coating	Alberola-Borras et al., 2018 [22]
	$Cs_x(MAFA)_{1-x}Pb(IBr)_3$	spin coating	

Figure 1 shows the large variations in the GWP estimates per kWh [kg CO2-eq/kWh] reported in the previous major LCA literature. We determined that these variations reflected different life cycle inventories and different parameters assumed in production and operation.

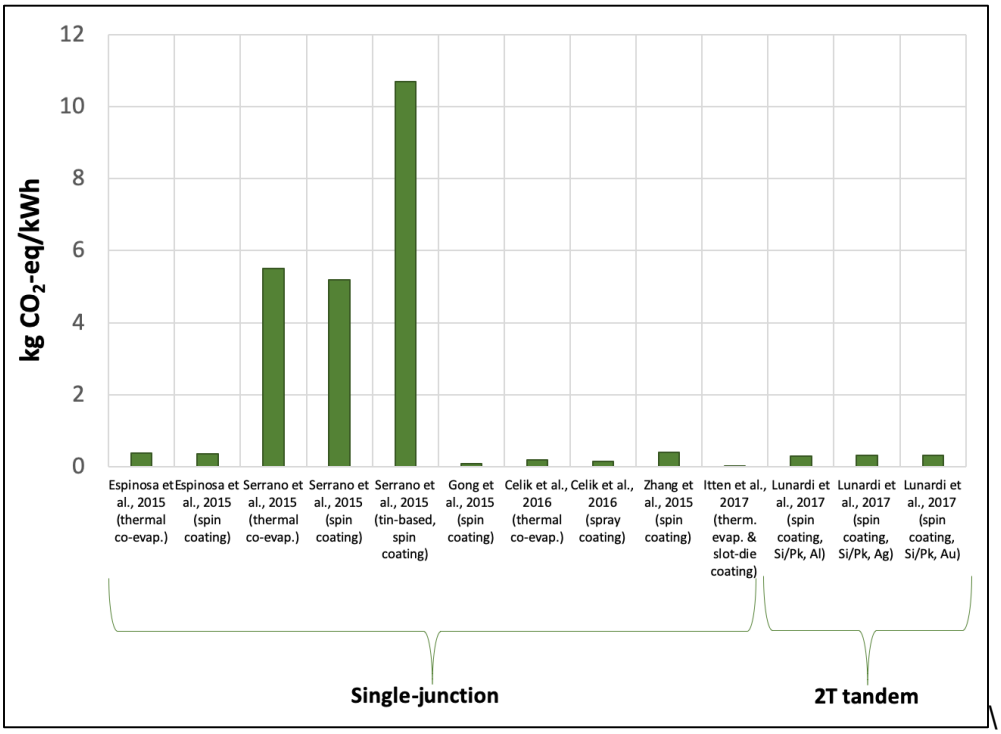

Figure 1: Comparison of Global Warming Potential results (kg CO2-eq/kWh) reported in LCA studies of single-junction and tandem perovskite PVs under different modelling assumptions (lifetime, performance ratio, efficiency, irradiation, and electricity grid mix) listed in Table 1.

The variability of modelling assumptions (e.g., power conversion efficiency, lifetime, performance ratio, irradiation, and electricity grid mix) used in major LCA studies is shown in Table 2. As an example, an examination of the GWP values reported by Serrano et al., 2015 [3], shows results ranging from 5.2 to 5.5 kg CO2-eq/kWh for the Pb-based perovskite devices, but 10.7 kg CO2-eq/kWh for the tin-based PSC device. This difference is mainly due to the lower power conversion efficiencies of the tin-based device (PCE of 6.4% vs 11.5-15.4%). Both numbers are artificially high as a life expectancy of only 1 year was assumed. Also, as shown in Figure 2 – which provides the comparison of GWP per kWp [kg CO2-eq/kWp] reported in previous LCA studies of single-junction and tandem perovskite PVs – the 2T tandem PV evaluated by Lunardi et al., 2017 [6] is reported to have an order of magnitude higher GWP impacts than the 2T tandem PVs reported by Celik et al., 2017 [5].

Table 2: Comparison of the modelling assumptions in previous LCA studies on single-junction and tandem perovskite PVs.

	Lifetime [years]	**Performance ratio**	**Irradiation [kWh/(m2*yr)]]**	**Efficiency [%]**	**Electricity grid mix**
Espinosa et al., 2015 [2]	15	0.8	1700	15.4 (thermal co-evaporation) 11.5 (spin coating)	Denmark electricity, low voltage
Serrano-Lujan et al., 2015 [3]	1	0.8	1700	15.4 (thermal co-evaporation) 11.5 (spin coating) 6.4 (tin-based, spin coating)	Denmark electricity, low voltage
Gong et al., 2015 [4]	2	0.8	1700	9.1	US electricity mix
Celik et al., 2016 [19]	5	0.75	1700	15 (thermal co-evaporation) 15 (spray coating)	US electricity mix
Zhang et al., 2015 [12]	5	0.75	1700	6.5	US electricity mix
Itten and Stucki, 2017 [20]	30	0.75	1700	18.3	European grid mix, low voltage
Lunardi et al., 2017 [6]	20	0.75	1700	24 (spin coating, Si/Pk, Al) 27 (spin coating, Si/Pk, Ag) 27 (spin coating, Si/Pk, Au)	-
Celik et al., 2017 [5]	5 (spin coating, CIGS/Pk) 5 (spin coating, Pk/Pk) 5 (spin coating, Si/Pk)	-	1700	19.5 (spin coating, CIGS/Pk) 21 (spin coating, Pk/Pk) 21 (spin coating, Si/Pk)	-

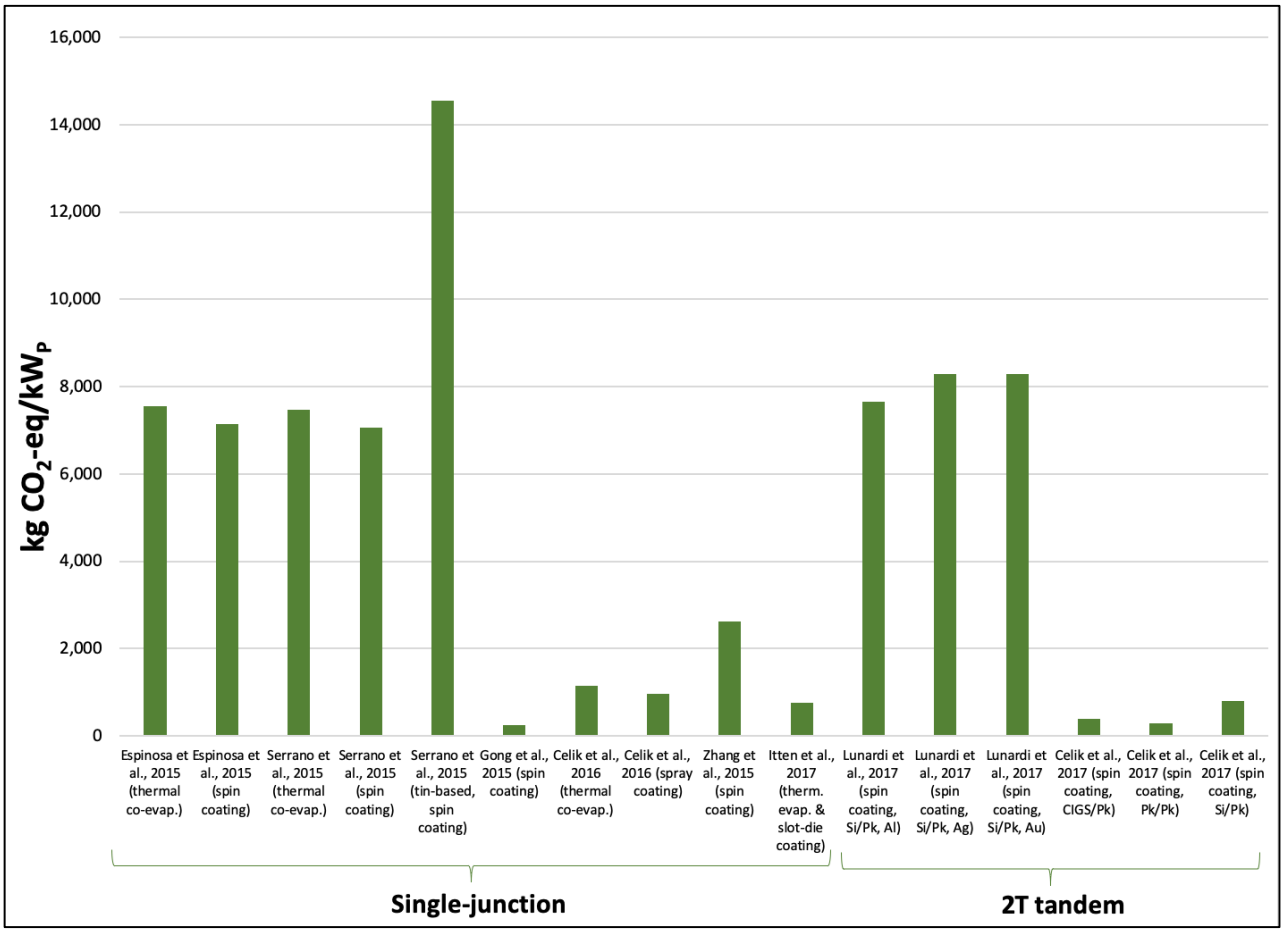

Figure 2: Comparison of Global Warming Potential results (kg $CO_{2\text{-eq}}/kW_P$) reported in LCA studies of single-junction and tandem perovskite PVs. (Note that "use factors" in the range of 0.15-10% were assumed in tandem PSC reported by Celik et al., 2017, but they were not used in the earlier estimates of single-junction PSC GHG emissions by the same author).

We normalized these results per m^2 of device, to remove the differences caused by different lifetimes, performance ratios, efficiencies, and irradiation levels assumed in the reported LCAs. Figure 3 shows the life-cycle cradle-to-gate GWP impacts [kg $CO_{2\text{-eq}}/m^2$] calculated per m^2 of single-junction and tandem perovskite devices. The remaining variations are due to the different materials used for manufacturing the perovskite layers, and different processes used for depositing the absorber layer; these are listed in Table 1. To further investigate the impacts associated with each PSC layer, we developed a comparison of cradle-to-gate GWP impacts (kg $CO_{2\text{-eq}}/m^2$) for the back contact, hole transport, absorber, electron transport, and top contact layers – as shown in Figure 4. The percentage contribution of each layer to the total GWP is shown in Figure 4a. The LCI given by Celik et al., 2016 [19] resulted to a high GWP % contribution assigned to the ETL layer; our investigation revealed that this was caused by inadvertently adding the Sn from the FTO into the ETL. We determined that the variations in GWP impacts are mainly caused by the difference in process energy assumed for the manufacturing of PSCs.

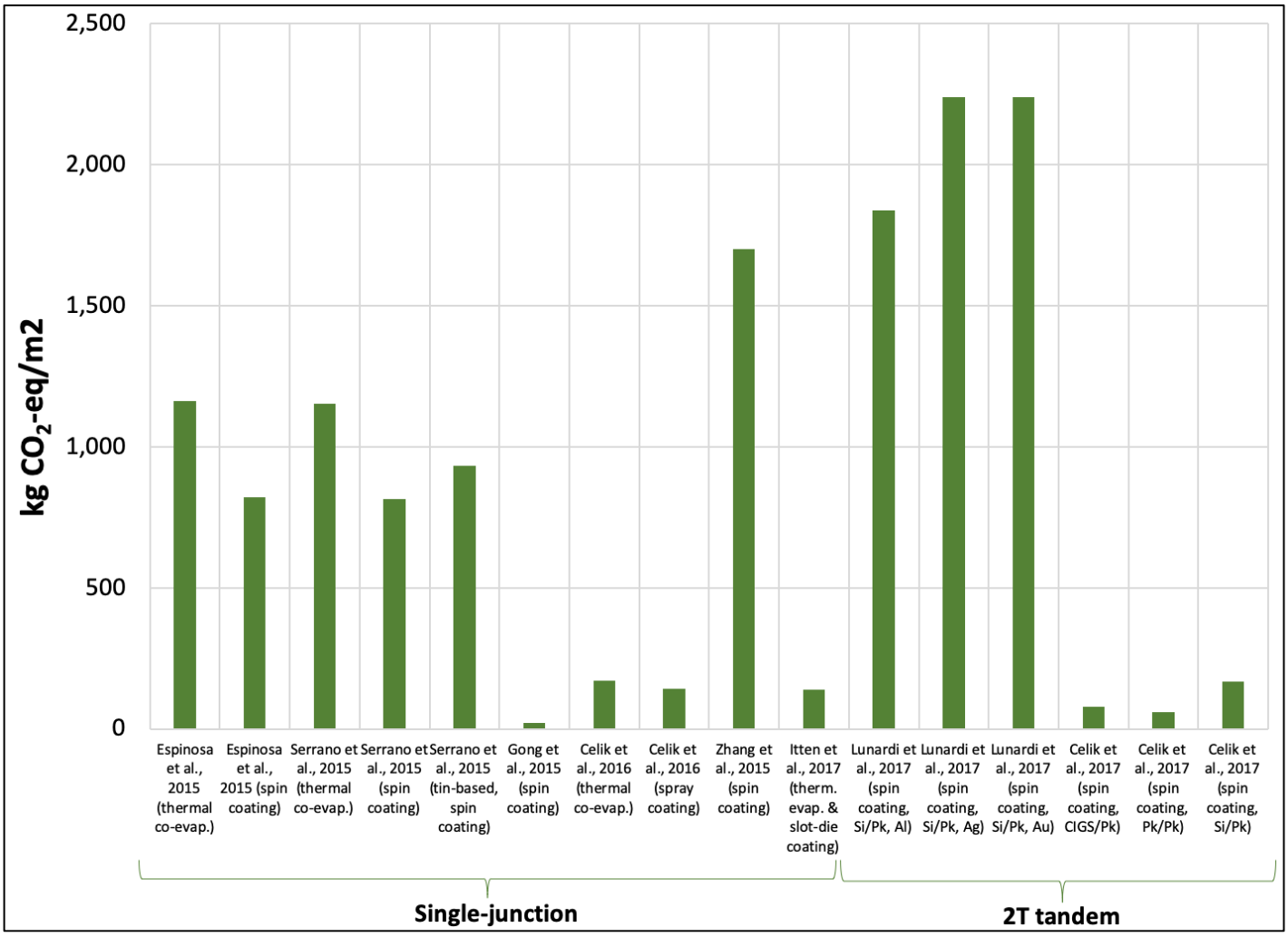

Figure 3: Comparison of Global Warming Potential results (kg $CO_{2\text{-eq}}/m^2$) reported in LCA studies of single-junction and tandem perovskite PVs. Impacts are presented per m^2. (Note that "use factors" in the range of 0.15-10% were assumed in tandem PSC reported by Celik et al., 2017 [5], but they were not used in the earlier estimates of single-junction PSC GHG emissions by the same author [19]).

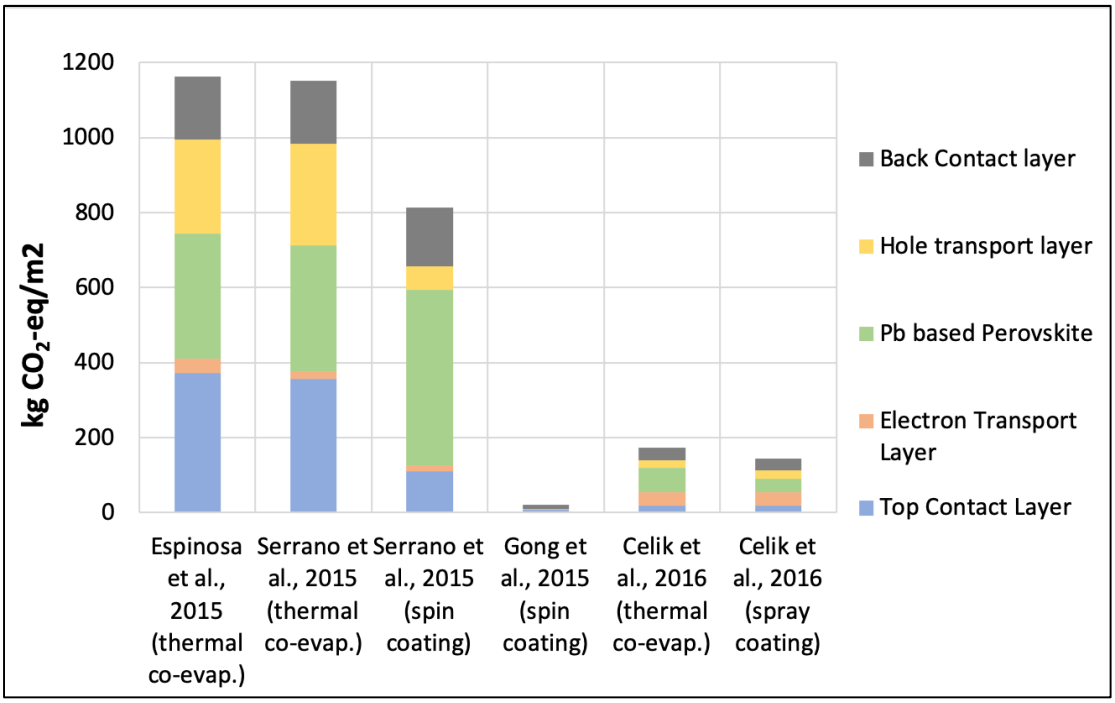

Fig. 4a: Comparison of Global Warming Potential results (kg CO2-eq/m^2) reported in previous LCA studies of single-junction perovskite PVs. Impacts are presented per m^2. The staked bars show the cradle-to-gate life-cycle individual contributions of each perovskite layer (back contact layer, hole transport layer, absorber layer, electron transport layer, top contact layer).

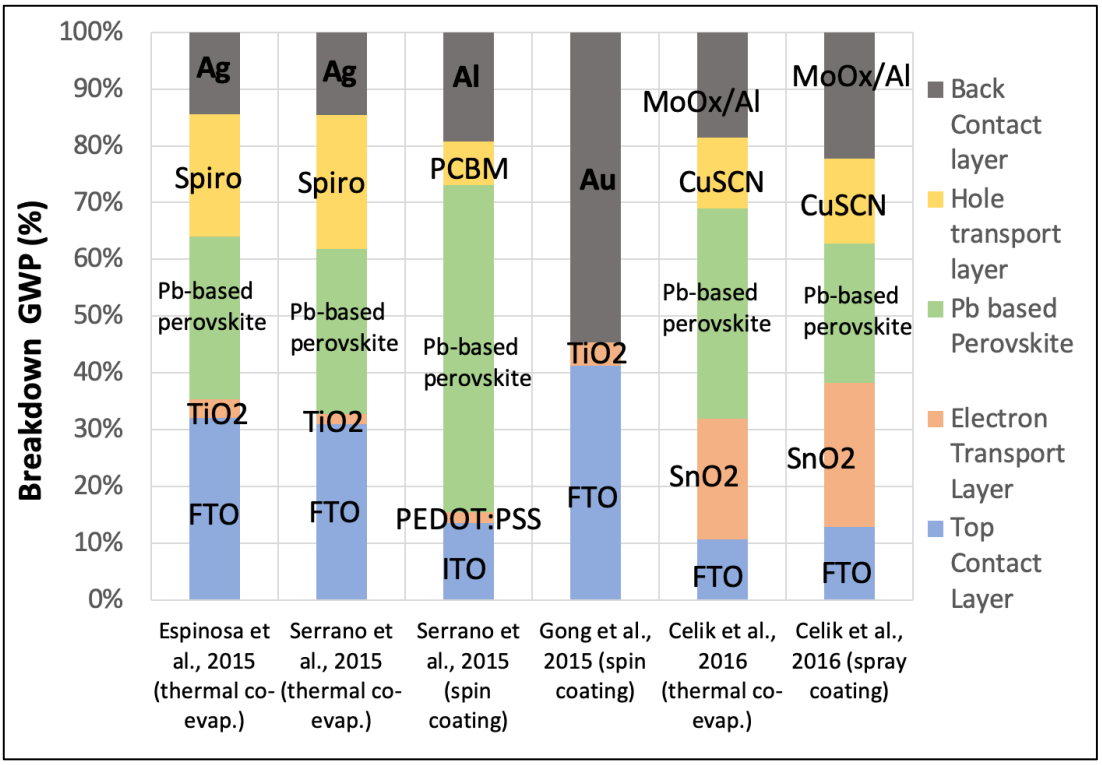

Fig. 4b: Breakdown (%) of Global Warming Potential results shown in Fig. 4a with details on the materials used for each layer of the single-junction perovskite devices.

As shown by the GWP breakdown in Figure 5, the electricity use is the major source of GHG emissions contributing 75 to 96% of the total emissions. Consequently, we investigated data and assumptions of direct electricity inputs for depositing each layer of the PSC device detailed in the supporting information of the reviewed articles.

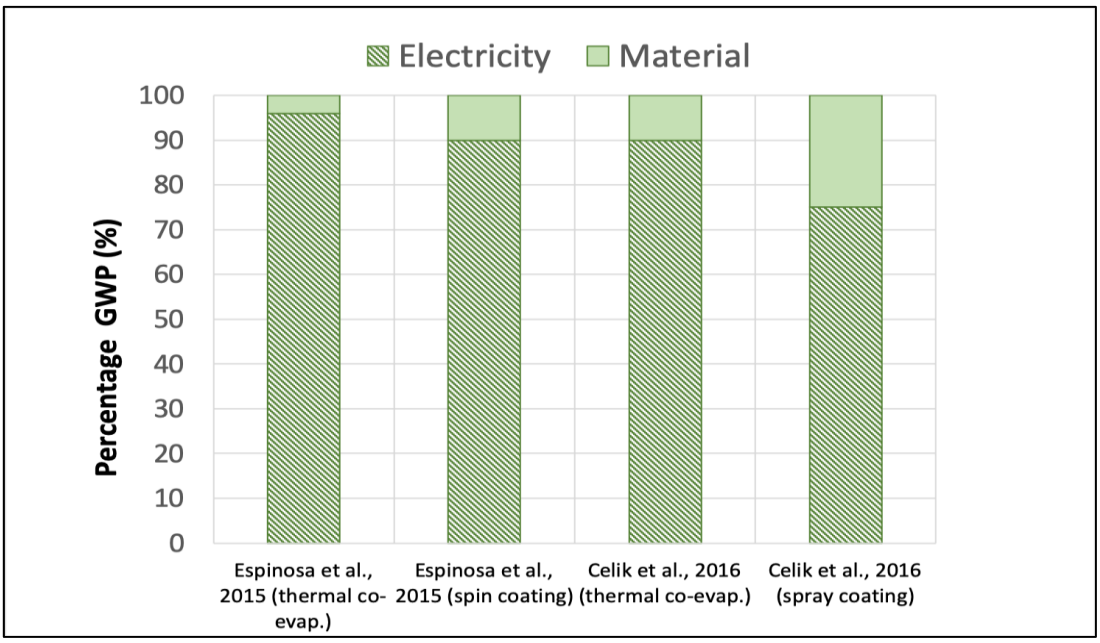

Fig. 5: Breakdown of Global Warming Potential (GWP) results from the life-cycle of single-junction perovskite PV module manufacturing in terms of electricity and material contributions.

Figures 6a and 6b show a comparison of the direct electricity inputs in terms of kWh/m^2 in PSC manufacturing reported in studies on single-junction perovskite PV LCA, where the stacked bars show the contribution of each layer. Gong et al., 2015 [4] estimated the direct process energy needed to fabricate a 1 m^2 single-junction perovskite module as 7.78 kWh (using spin-coating process), while Espinosa [2] found the same value as 1,080 kWh (also using spin-coating process), and 1,460 kWh (using thermal co-evaporation process). Such a big discrepancy requires a thorough examination; thus, we probed into the electricity input breakdowns behind these estimates (Figures 6a and 6b).

Gong et al., 2015 [4] evaluated the energy consumption by multiplying equipment power by the corresponding operation time (for ultrasonic cleaning, screen printing, sintering, spray pyrolysis); the energy consumption estimates for spin coating and thermal evaporation were obtained from Garcia-Valverde (2010) [23].

Specifically, 2.02 kWh/m2 is reported for the FTO top contact layer, assuming ultrasonic cleaning, screen printing, and sintering; 1.64 kWh/m^2 for the TiO_2 ETL, assuming screen printing and sintering; 0.58 kWh/m^2 for the Pb-based perovskite layer, including spin coating and sintering; 0.24 kWh/m^2 for the Spiro-MeOTAD HTL, assuming spin coating, and 3.30 kWh/m^2 is reported for the evaporation of the Au back contact layer.

Espinosa et al., 2015 [2] considered 142 kWh/m^2 for the ITO evaporation, 99 kWh/m^2 for the spin-coating deposition of the PEDOT:PSS ETL, 621 kWh/m^2 for the spin-coating deposition of the Pb-based absorber layer including annealing process, 0.5 kWh/m^2 for

the spin-coating of the PCBM HTL, and 216 kWh/m^2 for the evaporation in nitrogen glove box and vacuum of the Al back contact layer.

Comparing the electricity input breakdowns reported above, the main difference is the electricity estimation of the Pb-based absorber layer (0.58 kWh/m^2 in Gong et al., 2015 [4], and 621 kWh/m^2 in Espinosa et al., 2015 [2]), and it is mainly due to the spin coating and annealing processes. More specifically, for depositing Spiro-MeOTAD (HTL) by spin-coating, Gong et al., 2015 [4] estimated the electricity consumption to be 0.24 kWh per m^2, while Espinosa et al., 2015 [2] reported 276.38 kWh per m^2. Based on follow-up interactions with the authors, it became apparent than Gong et al underestimated the electricity consumption needed for the lab-scale spin coating deposition methods as they only considered the change in the mass and failed to consider the change in the kinetic energy requirement when the area of deposition was scaled-up.

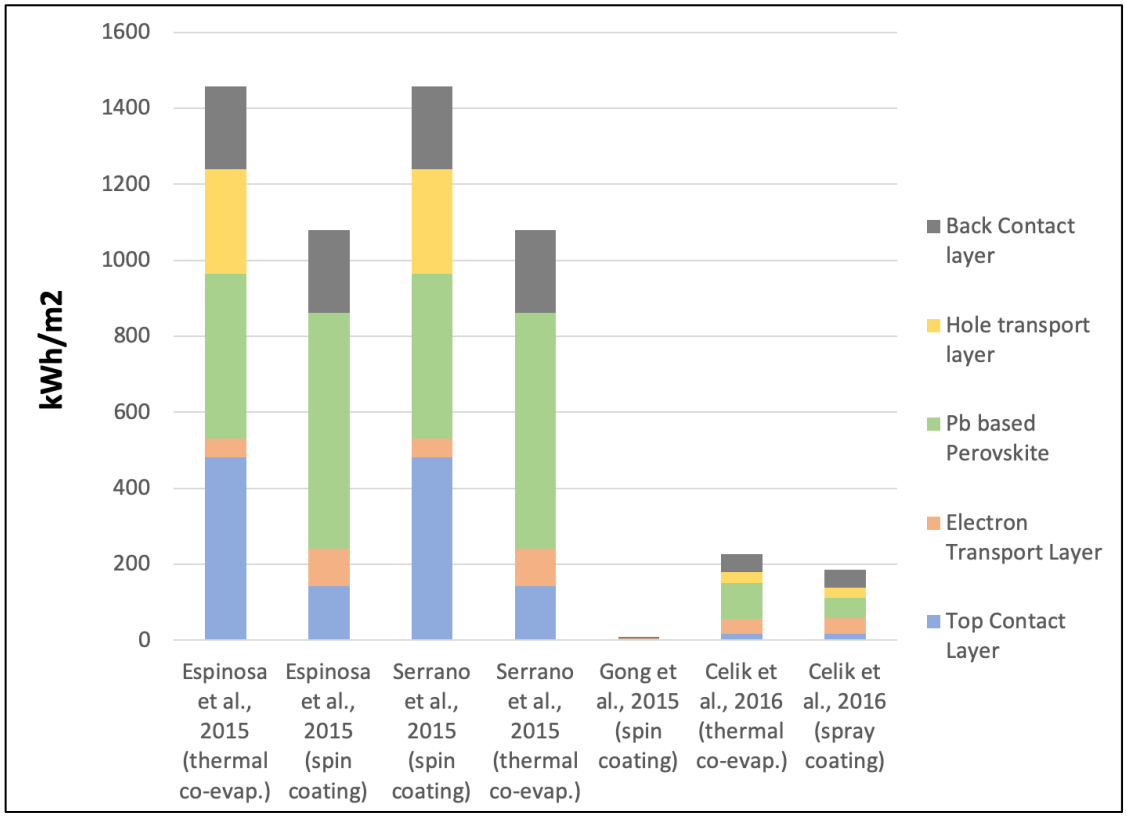

Figure 6a: Comparison of direct electricity inputs (kWh/m^2) in cell manufacturing reported in studies on single-junction perovskite PV LCA. The stacked bars show contributions of each perovskite layer (back contact layer, hole transport layer, absorber layer, electron transport layer and top contact layer).

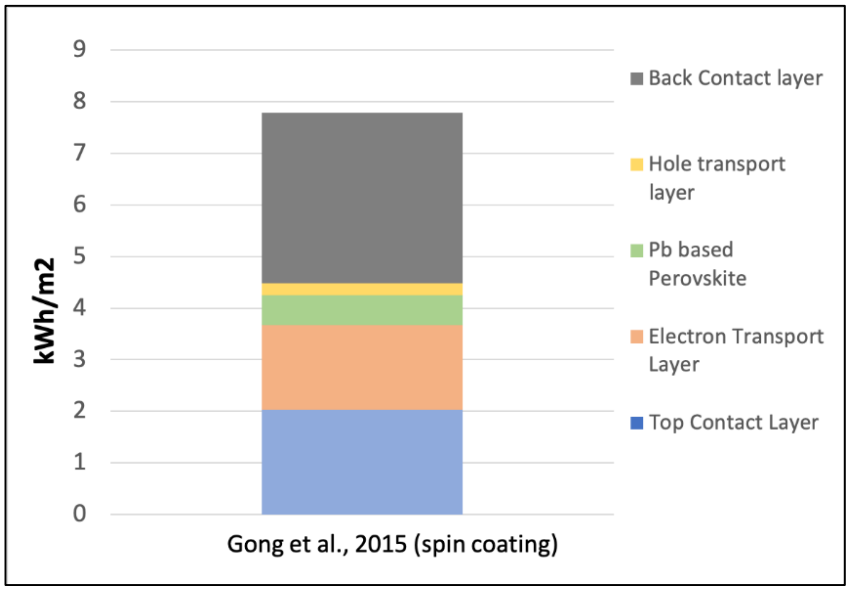

Figure 6b: Breakdown of direct electricity inputs (kWh/m2) in cell manufacturing reported Gong et al., 2015. The stacked bars show contributions of each perovskite layer (back contact layer, hole transport layer, absorber layer, electron transport layer and top contact layer).

The electricity inputs discussed above are also different in comparison with the direct electricity inputs required for manufacturing the two single-junction devices reported in Celik et al., 2016 [19]. As shown in Figure 6a, these are 225.55 kWh/m^2 for the thermal evaporation PSC device, and 184.72 for PSC, assuming spray coating as deposition process. Specifically, 16.38 kWh/m^2 is estimated for the FTO coated glass with ultrasonic process; 41.38 kWh/m^2 for the 60 nm SnO ETL, considering 1h pre-treatment stirring at 70°C, spray deposition, and 1h post treatment at 180°C; 6.11 kWh/m^2 for the 300 nm Pb-based absorber layer co-evaporation deposition with vacuum; 27.22 kWh/m^2 for the 700 nm CuSCN, including 1h pre-treatment stirring at room temperature, printing deposition, and post-treatment; 46.94 kWh/m^2 for the evaporation and vacuum of the 100 nm MoOox/Al back contact layer. Also, 52.77 kWh/m^2 is estimated as the direct electricity consumption for the spray deposition of 300nm Pb-based absorber layer, including 2h pre-treatment stirring at room temperature, and 30 min post treatment at 70°C. Comparing the electricity for depositing the Pb absorber layer, Celik et al., 2016 [19] reported 52.77 kWh/m^2 using spray coating process, considering 80% of deposition efficiency, while Gong et al., 2015 [4], reported only 0.58 kWh/m^2 using spin coating process. This is unjustified as spray coating has a much higher deposition efficiency than spin coating. As mentioned earlier, the later authors missed the change of kinetic energy; it seems that they also missed the energy required for pre-treatment and post-treatment. Figure 6a also shows the comparison between the two single-junction perovskite devices reported in Espinosa et al., 2015 [2]. In the first device (thermal co-evaporation), Spiro-MeOTAD was used as HTL requiring 276.38 kWh per m^2 as electricity input for the deposition, while 110 nm-thick PCBM was used as HTL in the second device (spin-coating) requiring 0.5 kWh/m^2 for the deposition, which is negligible. Thus, we concluded that Spiro-MeOTAD is the main contributor of the higher embedded energy in the two PSC devices.

In Figure 3, it is also worth noting the comparison between single-junction PSC GWP results reported by Celik et al., 2016 [19] with those calculated for the 2T tandem PSCs by Celik et al., 2017 [5]. The 2T tandem GWP impacts range from 60 to 168 kg CO2-eq/m^2, while the single-junction PSC GWP values are lower, ranging from 143 to 172 kg CO2-eq/m^2. The same counterintuitive comparison is shown in Figure 7. Specifically, the reported 2T tandem CED values is 419 MJ/m^2 for the perovskite/perovskite, 1,585 MJ/m^2 for the CIGS/perovskite, and 3,000 MJ/m^2 for the Si/perovskite, while the single-junction CED impacts vary from 2,550 MJ/m^2 (using spray-coating process) to 3,040 MJ/m^2 (using vacuum deposition). Contrary to expectations, the reported 2T perovskite/perovskite tandem has a CED that is 83% lower than the single-junction PSC deposited using spray coating, although the absorber deposition method used for the 2T tandem is spin-coating that has a worst deposition efficiency than spray coating (10% vs 80-95%). We deducted that the reason for this big difference is that the electricity consumption estimates in the 2T tandem devices incorporate “use factors”, representing a reduction of energy consumption in each process unit operation as is scaled from the lab to industrial production. Those were reported by García-Valverde et al. (2010) [23] to be 0.64% for evaporators, 0.2% for heaters, 10% for vacuum pumps, and 0.15% for spin coaters. We concur that in most cases, some type of energy discounting “use factors” should be used for extrapolating laboratory data to industrial production, but we are not convinced that a unit by unit extrapolation is appropriate as industrial process unit operations could be entirely different than laboratory synthesis steps (such as lab-scale spin coating).
Finally, figure 7 shows the breakdown of GWP results in terms of kg $CO_{2\text{-eq}}/m^2$ from the cradle-to-gate life-cycle of 2T tandem perovskite PV module manufacturing, where the stacked bars show the life-cycle individual contributions of silicon (Si), CIGS, and perovskite (Pk).

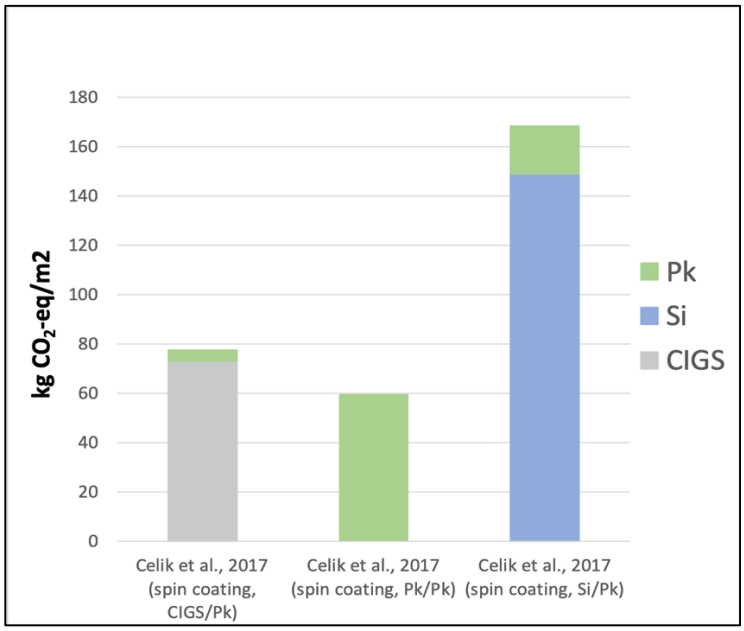

Fig. 7: Breakdown of Global Warming Potential results (kg $CO_{2\text{-eq}}$/m2) from the cradle-to-gate life-cycle of 2T Tandem perovskite PV module manufacturing. The stacked bars show the life-cycle individual contributions of silicon (Si), CIGS, and perovskite (Pk). Note in comparing this and Fig. 1 that “use factors” in the range of 0.15-10% were applied in Celik et al., 2017 [5].

Figures 8a and 9a illustrate respectively the human toxicity potential (HTP) results (carcinogenic effect) expressed in terms of comparative toxic unit for human toxicity impacts per m^2 ($CTUh/m^2$), and the freshwater ecotoxicity potential (ETP) impacts expressed in terms of comparative toxic unit for aquatic ecotoxicity impacts ($CTUe/m^2$), which are reported in previous LCA studies of single-junction and tandem perovskite PVs. Figure 8b and 9b provide the breakdown of those impacts, showing the contributions of each layer of the perovskite device.

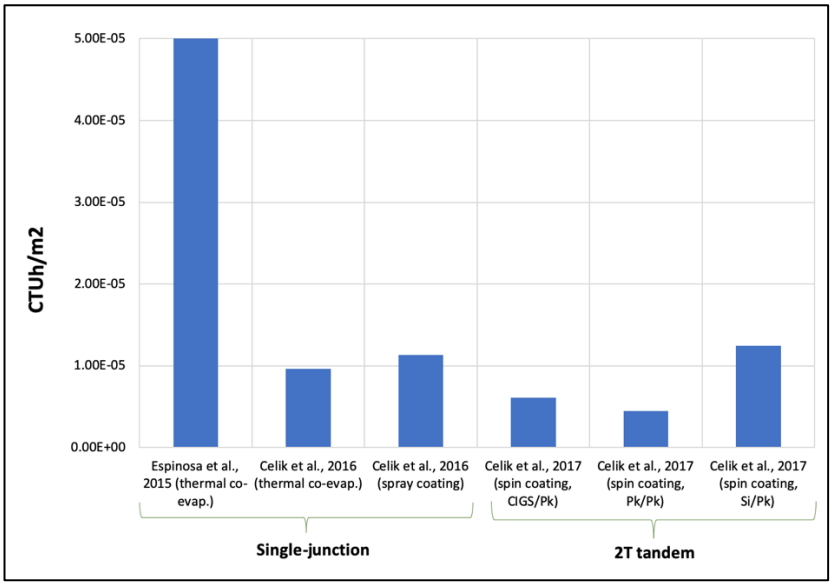

Figure 8a: Comparison of Human Toxicity Potential (HTP) [$CTUh/m^2$] results reported in LCA studies of single-junction and tandem perovskite PVs. Impacts are presented per m^2. Note that use factors in the range of 0.15-10% were used in 2T tandem reported by Celik et al., 2017 [5].

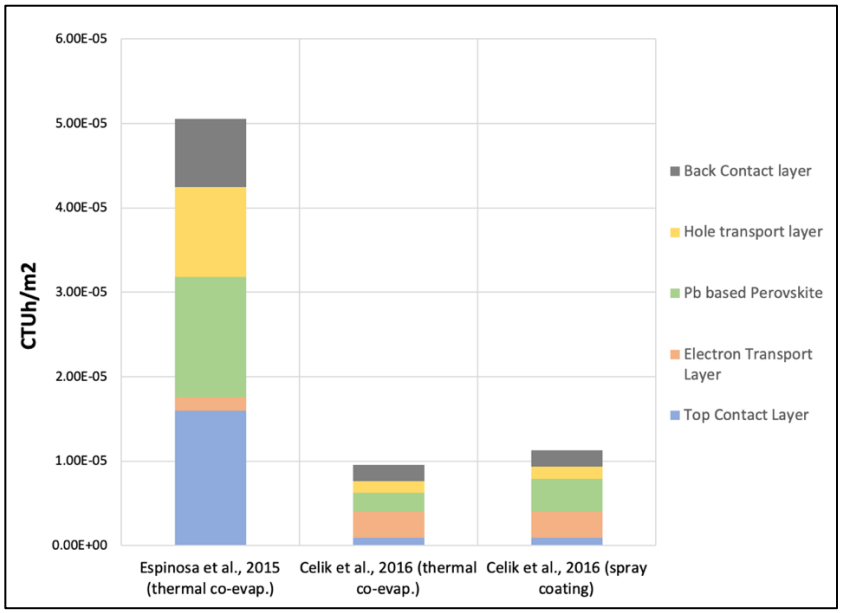

Figure 8b: Breakdown of Human Toxicity Potential (HTP) [$CTUh/m^2$] results reported in LCA studies of single-junction perovskite PVs. Impacts are presented per m^2. The stacked bars show contributions of each perovskite layer (back contact layer, hole transport layer, absorber layer, electron transport layer and top contact layer).

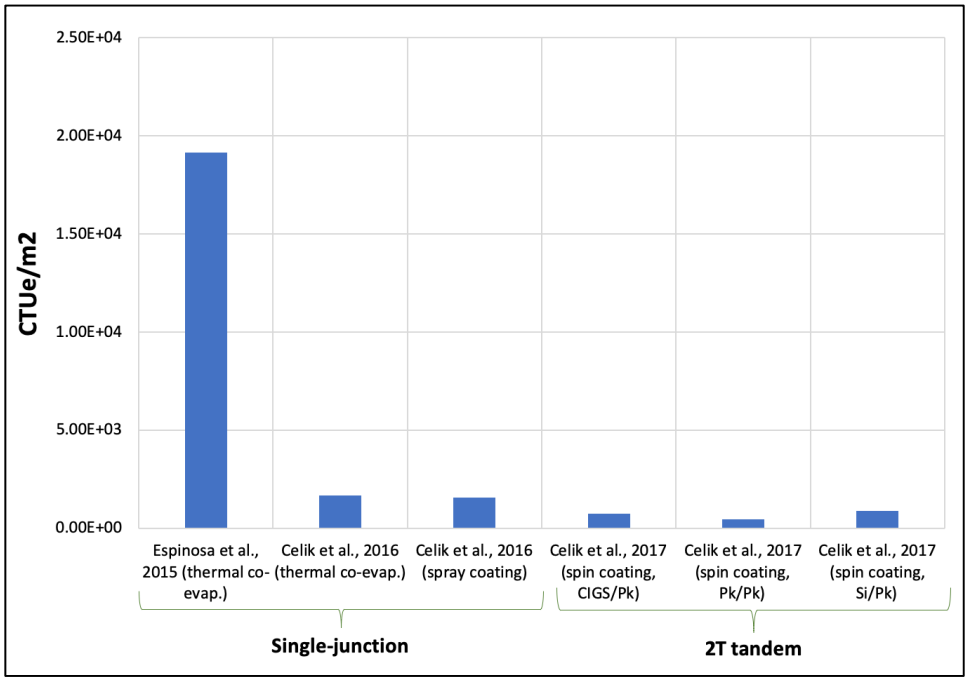

Figure 9a: Comparison of Ecotoxicity Potential (ETP) [CTUe/m^2] reported in LCA studies of single-junction and tandem perovskite PVs. Impacts are presented per m^2. Note that use factors in the range of 0.15-10% were applied in Celik et al., 2017 [5].

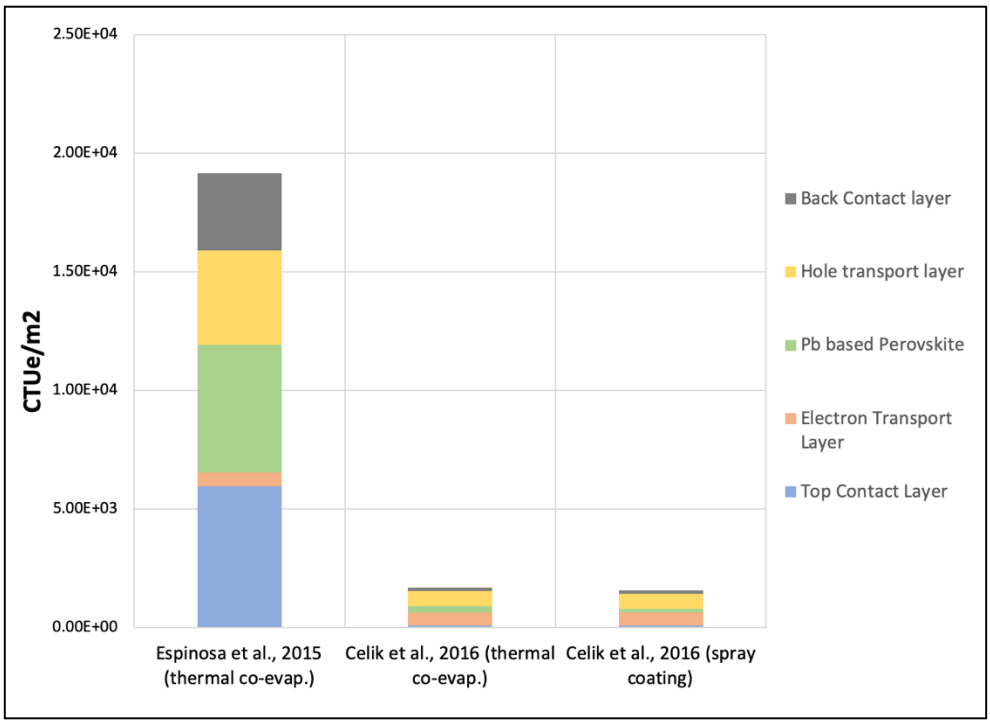

Figure 9b: Breakdown of Ecotoxicity Potential (ETP) [CTUe/m^2] results reported in LCA studies of single-junction perovskite PVs. Impacts are presented per m^2. The stacked bars show contributions of each perovskite layer (back contact layer, hole transport layer, absorber layer, electron transport layer and top contact layer).

From the ETP breakdown in Figure 9b, we noted that using copper thiocyanate as HTL in the PSCs reported by Celik et al., 2016 [19] is one of the main contributors for the ETP impacts, representing 37-40% of the total, while the contribution of SnO_2, assumed as ETL, ranges at 33-36%. Also, a similar trend is reported in HTP estimation, where the breakdown shows that SnO_2 ETL accounts for 28-32% of the total. However, after a further investigation of the life-cycle inventory reported in the supplementary information document by Celik et al., 2016 [19], we noted that the Sn-input estimation in the SnO_2 ETL mass life-cycle inventory is much higher than the expected quantity. Specifically, for a 60 nm SnO_2 ETL layer they reported that the Sn required is 5.70E-01 kg/m^2, but our own calculations based on stoichiometry and mass balances, show that it should be in the order of 10^{-4} per m^2 of PSC (assuming the same thickness, and SnO_2 density of 6.95 g/cm^3). Hence, the high contributions of the SnO_2 ETL in the resulting ETP and HTP life-cycle impacts calculated by Celik et al., 2016 [19] were highly overestimated. Our correspondence with the leading author revealed that this overestimate was the result of inadvertently adding to the ETL the amount of Sn mass contained in the FTO coated glass.
It is noted that the electricity process contributions range from 90 to 96% to the HTP results, and from 90 to 93% to ETP in Espinosa et al., 2015 [2], and consists of ~ 80% of the total in the devices analysed by Celik et al., 2016. Also, it is noted that “use factors” in the range of 0.15-10% are incorporated in the electricity required for manufacturing the 2T tandem devices reported in Celik et al., 2017 [5], as discussed in the previous section. Interestingly, Espinosa et al., 2015 [2] concluded that the contribution to HTP in the absorber layer is dominated by methylammonium iodide and its synthesis, and not by lead halides, which present less than 5% share of the overall impact.

6. Project Objectives:

Efficient, low-cost solar cells based upon lead halide perovskites have the potential to transform the US and global energy portfolio and improve energy security if they can be manufactured in an environmentally sustainable manner. However, although there is a plethora of articles on the efficiency of PSC in lab-scale testing, the Life Cycle Assessment literature before this project included only a couple of many PSC architectures and these do not distinguish which of the laboratory syntheses are scalable to commercial production [1].

To satisfy this need the project used a Life Cycle Analysis (LCA) framework to (i) characterize, (ii) quantify, and (iii) compare the life cycle health and environmental impacts of the most salient emerging scalable single-junction and tandem perovskite solar cell architectures, which have shown potential for achieving high-level power conversion efficiency (PCE), stability at the cell level, and scalable and reproducible processes. The project produced comparative evaluations of different single-junction and tandem PSC designs and production pathways, as well as comparisons between scalable perovskite with commercial PV systems that will inform decision makers and stakeholders. The results of the project would impact the future of PV manufacturing by providing industry, policy-makers, and academia with insights necessary to choose which perovskite solar

cell types cycles are environmentally sustainable in large scales of manufacturing and deployment.
Below is the list of the tasks included in the SOPO of the project all of which were fully attained. Details are discussed in the Projects Results and Discussion section of this report.

Task 1.0: Stakeholders Outreach (M1-M12)
Task 2.0: Development of scalable perovskite solar cell life cycle inventories (M1-M8)
Subtask 2.1: Compilation of single-junction perovskite solar cell material life-cycle inventories (M1-M4)
Subtask 2.2: Compilation of tandem perovskite most promising configuration life-cycle inventories (M5-M8)
Subtask 2.3: Analysis of the scalability of deposition methods (M3-M8)

GO/NO-GO DECISION POINTS:
a) Compilation of life-cycle inventories (LCIs) for three scalable single- junction and at least one tandem perovskite architectures, with data cross-referenced and examined with the NREL and the Stanford-Colorado R&D teams.
b) Identification and engagement of six to ten stakeholders in academia and industry representing various R&D and industry interests.
Task 3.0: Conduct Life Cycle Analyses (LCAs) to quantify the environmental footprint and potential impacts of the considered architectures (M6-M12)
Subtask 3.1: Impact analysis of single-junction perovskite PVs (M6-M10)
Subtask 3.2: Impact analysis of tandem perovskite PVs (M10-M12)
Task 4.0: Uncertainty Analysis and Comparison of perovskite solar systems with conventional technologies (M12-M15)
Task 5.0: Peer Reviews, Outreach and Dissemination (M14-M18)

7. Project Results and Discussion:

Task 1.0: Stakeholders Outreach (M1-M12)
Task Summary: *Identify major stakeholders in national labs, academia, material suppliers and process tool experts. Reach out to such stakeholders to cross-reference PSC configurations to be considered, and to get data and other information regarding the scalability and reproducibility of manufacturing processes*.
In the first stages of this project, we identified the following stakeholders, from which we received data and suggestions:

National Labs:
- Joe Berry, NREL
- Kai Zhu, NREL

Academia:
- Michael McGehee, U. of Colorado and Stanford U.,
- Jason Baxter, Drexel U.,
- Christophe Ballif, Ecole Polytechnique,
- Ilke Celik, University of Wisconsin – Platteville,

Industry/Tool Experts:

- Dirk Weiss, First Solar,
- Brett Kamino, CSEM,
- Chris Eberspacher, Tandem PV,

As perovskite development is very dynamic, during the course of our investigation we interacted with other stakeholders – listed below – from whom we received additional feedback and data.

- Colin Baile, TandemPV,
- BJ Stanbery, SivaPower,
- Ilke Celik, University of Wisconsin-Platteville,
- Stephan DeLuca, Energy Materials Corporation,
- Jinsong Huang, University of North Carolina at Chapel Hill,
- Yanfa Yan, University of Toledo,
- Zhaoning Song, University of Toledo,
- Yanfa Yan, University of Toledo,
- Rafael Garcia Valverde, Infinity PV and University of Cartagena,
- Nieves Espinosa, European Commission,
- Lucia Serrano Lujan, King Juan Carlos University
- Joseph Luther, NREL
- Rosario Vidal, Universitat Jaume I
- Pierre Verlinden, AMROCK Pty Ltd
- Werner Warmuth, PSE Projects GmbH

Overall, the main feedback we received from stakeholders are:

(i) Suggestions and review of the most promising perovskite single-junction and tandem architectures to be included in the project, including material and process industry scalability.
(ii) Energy data on roll-to-roll production.
(iii) Suggestions and review of process breakdown and scalability analysis of energy data from lab- to industrial-scale,
(iv) Suggestions and review of the updated material usage in perovskite-silicon tandem devices (such as silver and silicon),
(v) Review of our final material and energy life cycle inventories,
(vi) Suggestions and review on the assumed reference and future efficiencies of single-junction and tandem perovskite devices,
(vii) Verification of industrial relevance of considered solvents used in solution-based perovskite devices,
(viii) Review of our final life-cycle assessment results.

The major correspondence with those stakeholders and other LCA analysts is listed in the Appendices of previous reports.

Task 2.0: Development of scalable perovskite solar cell life cycle inventories (M1-M8)
Task Summary: A life cycle analysis framework typically entails the following four steps: 1) Goal and Scope definition, 2) Compilation of Life Cycle Inventory (LCI), 3) Impact analysis and evaluation, and 4) Interpretation of results [13-16]. For new technologies the LCI compilations is the most challenging task. It entails identification and quantification of all material and energy inputs, outputs and emissions in each of the stages of a life-cycle. Leveraging existing literature and industrial experience, we compiled life-cycle material, energy and emissions inventories for the production of promising architectures for PSCs tested at laboratory scale. We identified scalable fabrication methods as well as the most promising configurations and materials to be implemented at large-scale. Since there is not commercial production of PSC, a first phase of LCI compilation starts by reviewing all the material and energy data available in the literature, and identifying those that can apply to a large-scale industrial production.
Finally, we considered four single-junction PSC architectures, which include nine material layer composition alternatives, two encapsulation techniques, three different deposition process, and two different substrate types, as detailed into the following subtasks.

Subtask 2.1: Compilation of single-junction perovskite solar cell material life-cycle inventories (M1-M4)
Subtask Summary: We identified materials and configurations for each layer in the single-junction PSC, examining and comparing promising alternatives that have also shown a potential for large-scale production. For the first layer, also known as the top contact layer, we considered coated glass with fluorine doped tin oxide (FTO) and indium tin oxide (ITO). For the electron transport layer, we analyzed two options that are tin dioxide (SnO2) and fullerene derivative [6,6]-phenyl-C61 butyric acid methyl ester (PCBM). For the absorber layer we evaluated methylammonium lead halide (CH3NH3PbI3), deposited with three different methods (gravure printing, spray coating and vapor deposition). For the hole transfer layer, the most commonly used material at laboratory scale is Spiro-MeOTAD, which is very expensive and unstable. Thus, we examined alternative inorganic HTLs, which are copper thiocyanate (CuSCN) and nickel oxide (NiOx) as they can lead to high efficiency and better stability than Spiro-MeOTAD, and also low production cost. As back contact layer we avoided the use of gold (Au) – which is commonly used at lab-scale – and we considered two alternatives that are molybdenum oxide/aluminum (MoOx/Al) and silver (Ag) because they have a better chance to be deployed in large-scale production.
Also, we considered two encapsulation techniques, which are glass-PET (polyethylene terephthalate) for a roll-to-roll production and a glass-glass for rigid substrates.
Figure 10 shows a summary of our four single-junction perovskite architectures with details on each layer, material, thickness and deposition process.

PSC Layer	PSC RtR GP Encapsulation: Glass-PET		PSC SC alt 1 Encapsulation: Glass-Glass		PSC VD alt 2 Encapsulation: Glass-Glass		PSC SC alt 3 Encapsulation: Glass-Glass	
	Materials and thickness	Processes	Materials and thickness	Processes	Materials and thickness	Processes	Materials and thickness	Processes
TCL	FTO 500 nm	gravure printing cleaning	FTO 500 nm	oxygen plasma	ITO 110 nm	ultrasonication	FTO 500nm	oxygen plasma treatment
ETL	SnO2 60 nm	gravure printing annealing	SnO2 60 nm	spray coating annealing	SnO2 60 nm	spray coating annealing	PCBM 50 nm	spray coating annealing
Absorber	MAPbI3 300 nm	gravure printing annealing	MAPbI3 300 nm	spray coating annealing	MAPbI3 300 nm	evaporation vacuum	MAPbI3 300 nm	spray coating annealing
HTL	CuSCN 700 nm	gravure printing annealing	CuSCN 700 nm	spray coating annealing	CuSCN 700 nm	spray coating annealing	NiOx 60 nm	spray coating annealing
BCL	MoOx/ Al 100 nm	gravure printing annealing	MoOx/ Al 100 nm	evaporation vacuum	MoOx/ Al 100 nm	evaporation vacuum	Ag 100 nm	evaporation vacuum

Figure 10: Four single-junction perovskite architectures with details on each layer, material, thickness and deposition process.

Subtask 2.2: Compilation of tandem perovskite most promising configuration life-cycle inventories (M5-M8)

Subtask Summary: We reviewed several perovskite tandem architectures developed by the R&D community, which have the potential to enhance the PCE of solar cells beyond the Shockley-Queisser limit. Then we selected the most promising, replacing materials and processes that are not suitable for large-scale industrial. Specifically, we analyzed two devices, which are:

(i) A two-terminal (2T) Silicon-perovskite (2T Si-Pk) tandem, reported in 2019 by the McGehee's group [24].

(ii) A flexible all-perovskite tandem (2T Pk) device developed in 2019 by NREL, University of Colorado, and Stanford University [25].

In the 2T Si-Pk tandem, we replaced the lab-scale Si thickness (0.30 mm) with the commercial expected Si thickness (0.18 mm) and the float zone growth process with Czochralski process. The final 2T Si-pk architecture is shown in Figure 11a, in which each material, thickness, and processes is listed.

In the 2T all-Pk tandem we replaced gold (Au) with Ag and spin coating with spray coating, as shown in Figure 11b.

As encapsulation methods, we examined two types, which are:

- a glass-glass 2T all-perovskite tandem configuration, named "2T Pk tandem (a)",
- a glass-PET 2T all-perovskite tandem configuration, named "2T Pk tandem (b)".

As absorber layer for tandems, we analyzed double and triple cations, as shown in Figures 11a and 11b.

Materials and thickness	Processes
Ag wires	Thermal evaporation
Indium Tin Oxide (ITO) 50	Sputtering
SnO2 20 nm	Atomic layer deposition
PCBM 10 nm	Spray coating
LiF 1 nm	Thermal evaporation
$Cs_{0.17}FA_{0.83}Pb(Br_{0.17}I_{0.83})_3$ 350 nm	Spray deposition
PFN 1 nm	Thermal evaporation
Poly-TDP $(C_{22}H_{21}N)_n$ 5 nm NiOx 20 nm	spray coating spray coating
Indium Tin Oxide (ITO) 20 nm	Sputtering
i a-Si 5 nm / p a-Si 10 nm	Plasma-enhanced CVD
Si 0.18 mm	Czochralski
i a-Si 5 nm / p a-Si 10 nm	Plasma-enhanced CVD
ITO 80 nm Ag 100 nm	Sputtering Thermal evaporation

Materials and thickness	Processes
ITO 110 nm	Sonication and ozone treating
Poly-TDP $(C_{22}H_{21}N)_n$ 5 nm PFN-Br $(C_{56}H_{80}N_2.Br_2)_n$ 1 nm	Spray coating Spray coating
$FA_{0.6}Cs_{0.3}DMA_{0.1}PbI_{2.4}Br_{0.6}$ 300 nm	Spray coating
Lithium fluoride (LiF) 1 nm C_{60} 30 nm	Thermal evaporation Thermal evaporation
Polyethylenimine 1 nm	Spray coating
Aluminum-doped zinc oxide 25 nm	Atomic layer deposition
Indium Tin Oxide 5 nm	Sputtering
PEDOT:PSS 20 nm	Spray coating
$FA_{0.75}Cs_{0.25}Sn_{0.5}Pb_{0.5}I_3$ 850 nm	Spray coating
C_{60} 30 nm	Thermal evaporation
Bathocuproine (BCP) 6 nm	Thermal evaporation
Ag 100 nm	Thermal evaporation

Figure 11a (left): 2T Silicon/perovskite tandem solar cell architecture based on McGehee, 2019 [24] and adapted with our changes for scalability, replacing (i) the lab-scale Si thickness (0.30 mm) with the commercial Si thickness (0.18 mm), and (ii) float zone growth with Czochralski process.
Fig.11b (right): 2T all-perovskite tandem architecture with materials, thicknesses and processes for each layer. Based on Palmstrom at al., 2019 [25] and adapted for scalable materials and processes, replacing (i) Au with Ag and (ii) spinning with spray coating.

Subtask 2.3: Analysis of the scalability of deposition methods (M3-M8)
Subtask Summary: A key factor for transitioning from laboratory to factory scale is the scalability of the deposition methods of the perovskite solar cell, then we evaluated and compared various alternatives, which include two main strategies that are vapor-phase and solution-phase depositions. For solution-based deposition methods, we compared spin coating, blade coating, slot die coating, spray coating, gravure printing, inkjet printing, screen printing, and electrodeposition in terms of their material waste and potential scalability. We concluded that spin coating is not viable for industrial scale production due high material waste (90%). Among these alternatives, we focused in particular on the most promising solution-based techniques for the scale up of PSC manufacturing, which are spray coating and gravure printing. We considered a roll-to-roll perovskite production using gravure printing for all the layers – including the top contact layer and back contact layer – and a flat panel processing, using spray coating. Finally, we considered also vapor based deposition method for comparison. DONE

GO/NO-GO DECISION POINTS*: a) Compilation of life-cycle inventories (LCIs) for three scalable single- junction and at least one tandem perovskite architectures, with data cross-referenced and examined with the NREL and the Stanford-Colorado R&D teams*.
We exceeded the threshold of Go/No-Go Decision Point; We completed LCIs (and LCAs) for 4 single-junction and 3 tandem perovskite technologies

b) Identification and engagement of 6 to 10 stakeholders in academia and industry representing various R&D and industry interests.

We engaged 24 stakeholders in this project, as listed in section 7 pp. 18-19 of this report.

Task 3.0: Conduct Life Cycle Analyses (LCAs) to quantify the environmental footprint and potential impacts of the considered architectures (M6-M12)

Task Summary: We performed LCAs to quantify and compare the life cycle impacts of four scalable single-junction and three tandem perovskite solar cell architectures. The perovskite PV systems were evaluated in comparison with commercial PV technologies that are single-crystalline (sc-Si), cadmium telluride (CdTe), copper indium gallium selenide (CIGS). We provided energy and environmental impacts, measured by Cumulative Energy Demand (CED), Global Warming Potential (GWP), Ozone Depletion Potential (ODP), Acidification Potential (AP), Human Toxicity Potential (HTP), Eco-toxicity Potential (ETP), Abiotic resource Depletion Potential (ADP), Photochemical Oxidation Potential (POP), and Eutrophication Potential (EP). In addition to those, we calculated the Energy Pay-Back Time (EPBT) and the Energy Return On Investment (EROI) for complete perovskite PV systems – including the balance of system components – installed at three irradiation levels and considering reference and future potential module efficiencies. Finally, a sensitivity analysis on perovskite lifetime was performed, considering 10, 20 and 30 years.

The detailed LCA results in terms of energy and environmental impacts are included in our manuscript that is currently under review – titled "*Life-cycle energy demand and carbon emissions of industrial production of single-junction and tandem perovskite PV*" – submitted to the Energy and Environmental Science Journal (IF 30) on October 10, 2020. Other LCA results in terms of toxicity and resource depletion are included in a manuscript in preparation.

Same samples of our LCA results are provided below.

Figure 12 shows the Global Warming Potential [kgCO2eq/m2] comparison between four single-junction and three tandem perovskite devices with conventional PV panels with breakdown of solar cell, encapsulation and aluminum frame. GWP results range from 16 kgCO2eq/m2 to 163 kgCO2eq/m2. It is noted that the solar cell contribution (including the sum of all the layers) is higher than encapsulation and aluminum framing in PV devices, with PSC RtR GP being a notable exception.

Figure 13 shows the CED results in terms of their life-cycle MJ per kWp rated output for four single-junction and three tandem perovskite architectures, compared to sc-Si, CdTe and CIGS panels, using both current reference and future potential module efficiencies listed in the figure caption. Assumed efficiencies are based on the latest "Photovoltaics Report 2020" released by the Fraunhofer Institute for Solar Energy Systems [26], and on the "Best Research-Cell Efficiency Chart" provided by the National Renewable Energy Laboratory (NREL) [27].

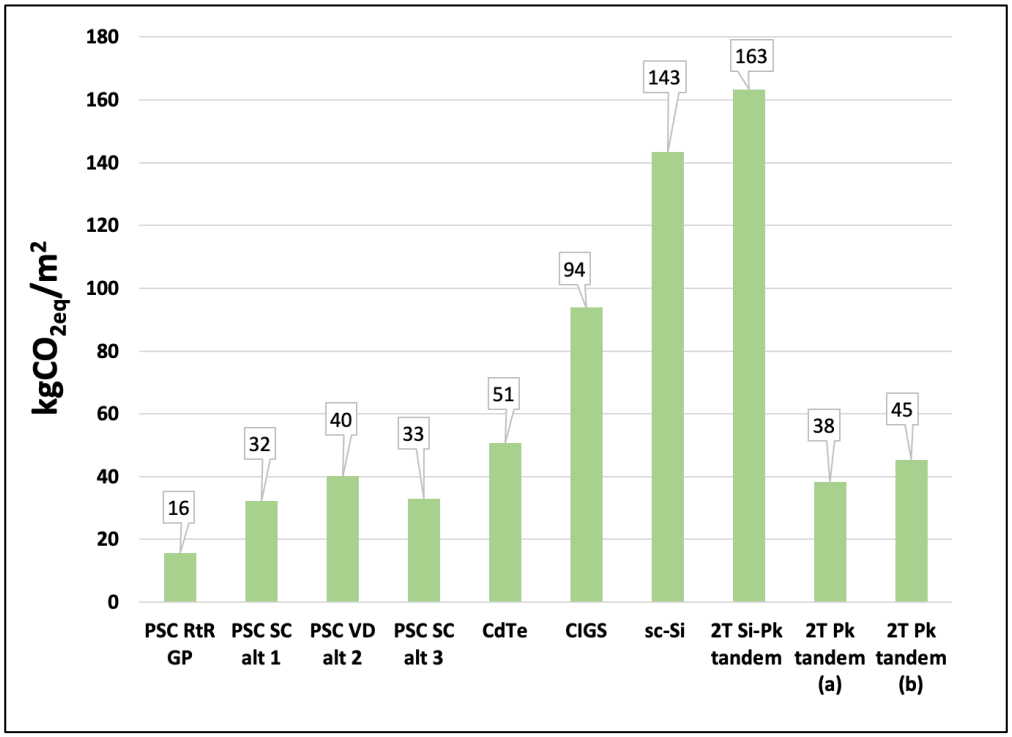

Figure 12: Global Warming Potential [$kgCO_{2eq}/m^2$] comparison between perovskite and conventional PV panels.

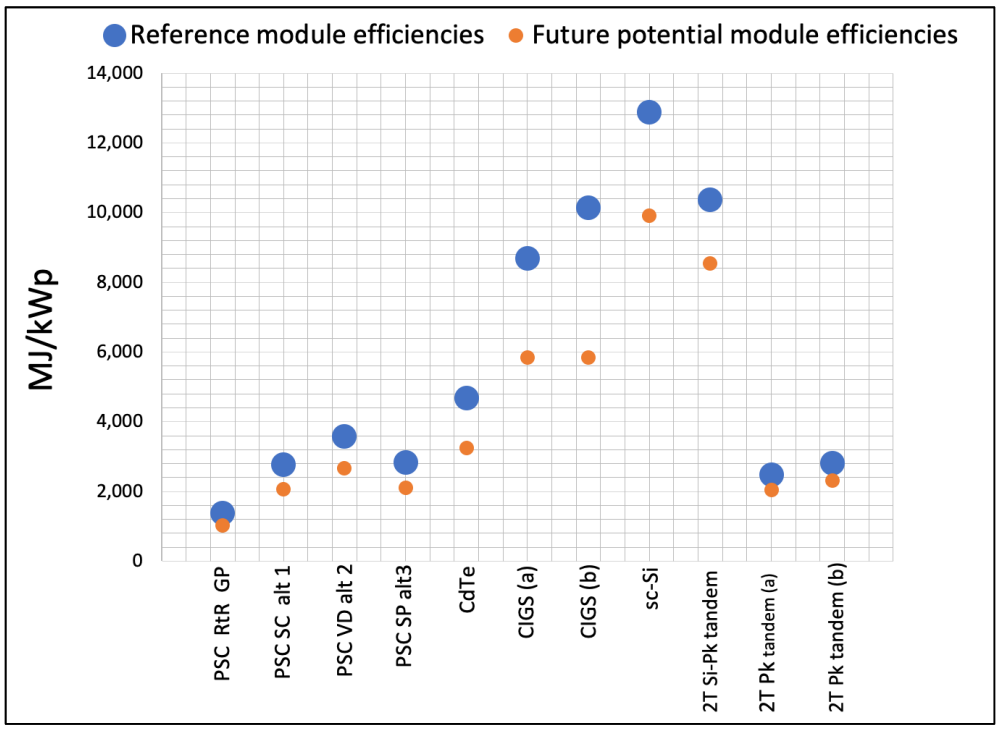

Figure 13: Cumulative Energy Demand [MJ/kWp] comparison between perovskite and conventional PV panels. Reference and future potential module efficiencies are respectively: 19.3% and 26% for single-

junction perovskite; 18% and 26% for CdTe; 17.5% and 126% for CIGS(a) and 15% and 26% for CIGS(b); 20% and 26% for sc-Si; 28% and 34% for perovskite tandems [26-27].

Subtask 3.1: Impact analysis of single-junction perovskite PVs (M6-M10)
Subtask Summary: We characterized and quantified the life cycle impacts of four scalable configurations of single-junction perovskite PV systems.
As an example, our estimated CED values range from 265 MJ/m2 for the roll-to-roll single-junction perovskite fabricated using gravure printing (PSC RtR GP) to 691 MJ/m2 for the perovskite architecture in which vapor deposition is used for the absorber layer (PSC VD Alternative 2). Our LCAs show that Ag is more energy demanding than MoOx/Al used as back-contact-layer materials. Results also show that encapsulation is the major contributor in comparison with the other perovskite layers, ranging from 37% to 61% of the total energy footprint. Regarding the top contact layer options, our LCAs show that FTO is less impactful in terms of both energy demand and carbon emissions compared to ITO-based layers, especially when FTO is produced using RtR gravure printing.
One of the main findings of our LCA is that perovskite lead-based absorber layer does not represent a major contributor in all the analyzed alternatives, both in terms of carbon emissions and cumulative energy demand, ranging from about 1% (using spray coating) to 20-23% (using vapor deposition).

Subtask 3.2: Impact analysis of tandem perovskite PVs (M10-M12)
Subtask Summary: We characterized and quantify the life cycle impacts of two three promising two-terminal tandem perovskite PV systems (one of which is silicon-perovskite and two of which are all perovskite), and we compared results with the single-junction perovskite and commercial PV systems.
Our LCA contribution analysis show that the main contributions in both all-perovskite devices consist of the encapsulation, the Ag back-contact layer and the top contact layer (ITO). Overall, the CED values range from 696 MJ/m2 to 790 MJ/m2 for the 2T all-perovskite tandem alternatives – depending on the encapsulation techniques. The Si-Pk tandem CED is estimated to be 2,903 MJ/m2, with the Czochralski process being the main contributor (77% of the total).

Task 4.0: Uncertainty Analysis and Comparison of perovskite solar systems with conventional technologies (M12-M15)
Sensitivity and uncertainty analyses were conducted to evaluate major parameter influences. The energy footprint and environmental impacts associated to perovskite PV systems were compared and contrasted with established PV technologies, using LCA and Net Energy Analysis to inform the debate on Energy Return on Investment (EROI), based on previous work by the authors and other published studies [28-34].
For comparison with crystalline-silicon PV systems, we used updated 2020 data on silicon PV life cycle inventory released by the International Technology Roadmap for Photovoltaics (ITRP) [35], as integration to the IEA 2015 LCI [36], Specifically, we updated the Si usage – which was 1.58 kg/m2 for sc-Si and 1.02 kg/m2 for mc-Si [36], and kerf loss of 145 µm per cut from multi-wire slurry-based sawing. The new data show

that the Si usage ranges from 0.55 kg/m2 to 0.58 kg/m2, and the kerf loss for diamond wire cutting is 70 µm [35].
Our performed sensitivity analysis is based on perovskite lifetime and one of our findings show that RtR single-junction perovskite and all-perovskite tandem PV systems could reach the same EROI as that of crystalline-based PV systems within 12 years of life, while the perovskite systems produced using spray coating on rigid substrates would require a 15-yr life to match the EROI of 30-yr lasting silicon PV modules – as shown in Figure 14.

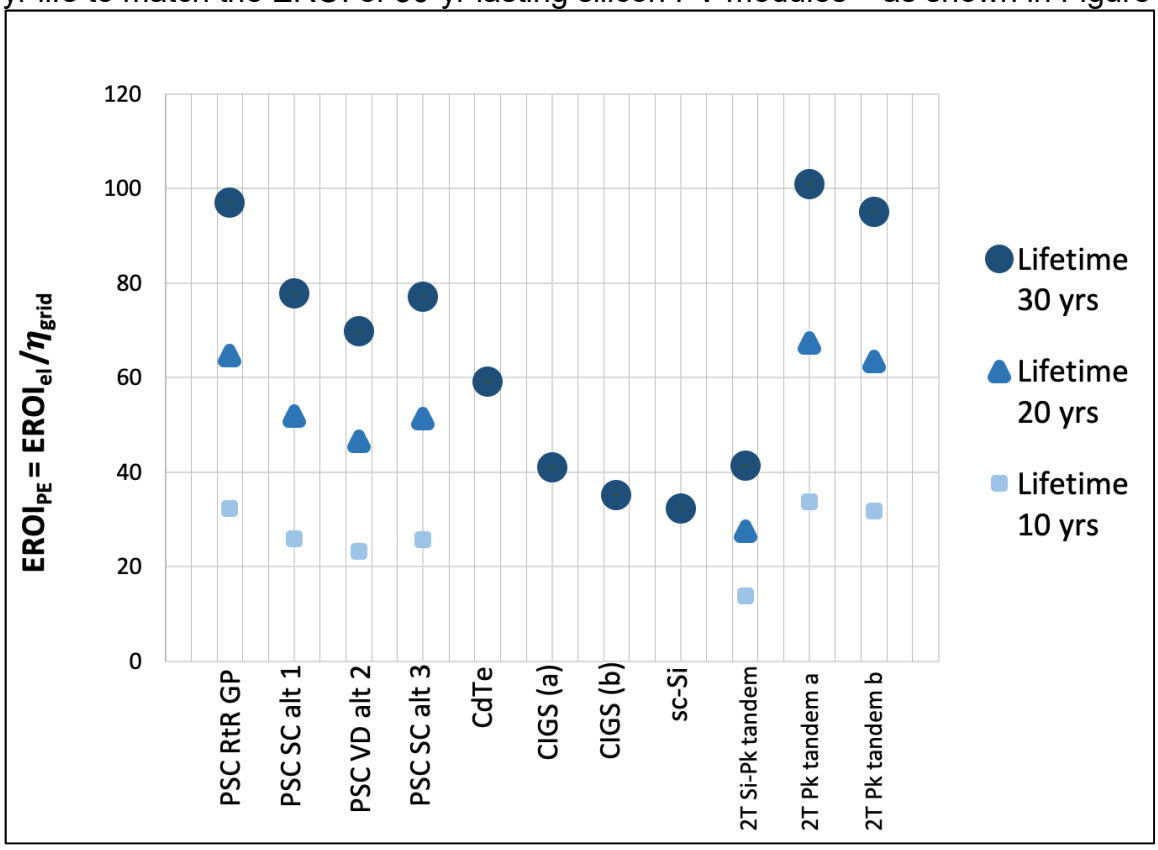

Figure 14: Energy Return on Investment in terms of primary energy ($EROI_{PE}$) comparison between four single-junction and three tandem perovskite systems with single-crystalline, CdTe, and CIGS PV systems. Results include BOS. ηG: 0.3. PR: 0.85 [26]. Irradiation: 1,800 kWh/(m^2*yr). Sensitivity analysis on perovskite lifetime (from 10 to 30 years).

EPBT results range from 0.3 to 0.4 years for the single-junction perovskite and all-perovskite tandem systems and 0.7 years for 2T Si-pk tandem systems, compared to 0.5 year for CdTe, 0.7-0.8 yr for CIGS, and 0.9 yr for sc-Si. It is noted that the listed values include BOS contributions, assume 1,800 kWh/(m^2*yr) as latitude-tilt global irradiation, 0.85 as performance ratio and η_G of 0.30 as grid efficiency.
Regarding uncertainty analysis, we performed life cycle processes in SimaPro software with the following main types of uncertainty: (i) variation in the data, and (ii) data correctness (representativeness). Regarding the foreground electricity data required for manufacturing 1 m^2 of PSC we addressed the uncertainties considering both primary and secondary life cycle inventory data sources.
The primary data source consists of new energy electricity data on roll-to-roll (RtR) gravure printing, which were derived from existing commercial eight-station RtR printing

tolls running 24/7 at 30 m/min – corresponding to 45m^2/min of PSC production with a 1.5m wide web moving at 30m/min. Assuming PPV efficiencies of 18-20% this production would correspond to 3-4 GW/yr of PSCs. We verified the data validity with our review of previous literature studies on organic solar cells [23-37].

Also, with the aim of providing results that are more representative as possible of the US geographical area we used the US electricity grid mix in the databases, which is named "*WECC US only*". The secondary data source for electricity consumption consists of our estimations based on the rated power of the equipment, the required time, and use factors. Our estimates have been validated considering the stakeholders involved in the project, and our comprehensive literature review on the topic, cross-referencing each source of data. The latter approach has been used also for estimating the foreground material inventory, considering the stakeholder suggestions, applying stochiometric and mass calculations, and cross-referencing all the identified source of information. The geographical area that has been chosen for the processes is named "*GLO*", which means a global representation. The largest and more impactful sources of uncertainty in the background data were addressed using the latest Ecoinvent database (v.3), which includes four libraries that are 1) *attributional unit*, 2) *attributional system*, 3) *consequential unit*, *consequential system*. We modeled the "*attributional unit*" processes because they have been developed with a specification of uncertainty. Specifically, each "*attributional unit*" data point includes uncertainty information. The resulted value can be interpreted as the "*best guess*" value, and it is determined by sampling the mean value of a (log)normal distribution that are characterized by a standard deviation. A typical property of a lognormal distribution is that the square of the geometric standard deviation covers the 95% confidence interval. Then, a square geometric standard deviation of 1.2 means about 95% of all measured values are between the mean value times 1.2 and the mean value divided by 1.2. If the square of the geometric standard deviation is equal to 1.0, there is no variation (all measured values are the same). In a normal distribution, the 95% confidence interval is found between two times the standard deviation above and below the mean.

Also, the processes are listed representing national, regional or global markets for each product. We used "global market processes" that include inputs for production in several countries as well as inputs for transport processes. When "*global market processes*" was not available in the database, we used "*RER market processes*" that represent European average production or "*ROW market processes*", consisting of *Rest of The World* average production.

Regarding the impact assessment method data uncertainty, we used three LCA methods, which are 1) Cumulative energy demand (single issue), 2) CML developed by Leiden University [38], and USEtox [39-40] for reducing the uncertainties associated with the method assumptions. In particular, for toxicity indicators (HTP, ETP) we applied both methods, CML and USEtox, which provide results expressed in different units, in order to verify the potential variations in the results.

Regarding the characterization factor uncertainty, we identified which are the assumptions behind each method (i.e., characterization factors associated with each element taken into the account) and as result we found that the major uncertainties are associated with the toxicity indicators. As a consequence, we probed into details for those indicators using both methods (CML and USEtox). Finally, an important LCA tool we

applied in understanding the uncertainty of our results is the use of contribution analysis in order to identify which processes are playing a significant role in our results.

Task 5.0: Peer Reviews, Outreach and Dissemination (M14-M18)
We disseminated results of our project to stakeholders and the general public, at IEEEPVSC 2019, popular magazines, and with two journal publication. These papers are listed in section 8 below.

8. Significant Accomplishments and Conclusions:

This project research identified challenges for fabrication transitioning from laboratory to sustainable industrial production, and contributed to the discipline of Life Cycle Analysis by developing new life-cycle inventory (LCI) data for scaling to industrial production most promising four (4) single-junction and three (3) tandem perovskite technologies. The environmental impact of these technologies was evaluated using a consensus LCA framework. This work lays the foundation for sustainability investigations of large-scale production and deployment of PSC.
The project has produced four published products, which are three journal papers, one conference proceedings paper and one popular magazine article; also, we will submit another manuscript (which is in preparation) focused specifically on toxicity and resource depletion results, with the aim of providing insights into the methodological uncertainties.

These papers with salient highlights are listed below:

- Leccisi, E. and Fthenakis, V., 2020. Life-cycle environmental impacts of single-junction and tandem perovskite PVs: A critical review and future perspectives. *Progress in Energy 2,* 032002, https://doi.org/10.1088/2516-1083/ab7e84. [41]

Credible LCA studies require actual process-based material, energy and emissions data, which may not exist before the technologies are commercially produced, thus, the perovskite LCA literature is based on linear extrapolations of laboratory data. In this paper we critically reviewed the PSC LCA literature, explain the reasoning for a wide divergence of results, and determined which data apply to scalable industrial production, materials and processes. Our investigation probed into the formulation of each layer of a PSC device, and its potential for industrial scale fabrication. We found that electricity use is the main contributor to reported LCA results, explaining the large difference, ranging from 7.78 kWh to 1,460 kWh/m2, among various studies. Subsequently, we identified and discuss methodological errors in some of these estimates. In terms of life-cycle toxicity most of the reviewed LCA studies do not attribute any major overall toxicity impact to the presence of lead in the PSC devices. We also reviewed and critiqued studies describing "worst-case" scenarios of accidental release of lead into the environment, and, in spite of statements in those studies, we found them to be inconclusive.

- Leccisi E. and Fthenakis V., Critical Review of Perovskite Photovoltaic Life Cycle Environmental Impact Studies, 2019 IEEE 46th Photovoltaic Specialists Conference (PVSC), Chicago, IL, USA, 2019, pp. 1-6, doi: 10.1109/PVSC40753.2019.9198977. [42]

This paper investigates a promising organic-inorganic lead halide perovskite solar cell (PSC) architecture in terms of its potential life-cycle environmental impacts. We critically reviewed the validity of assumptions and the results of previously published studies that were entirely based on data from laboratory PSC fabrication. As great challenges remain in scaling up devices from laboratory scale to large-area module manufacturing, we focus this investigation on identifying materials and processes that have a good scalability potential and minimum possible environmental footprints. Then, we conducted a first, preliminary environmental life-cycle analysis in terms of global warming potential (GWP) and acidification potential (AP) while discussing the scalability of associated manufacturing processes.

- Baxter J., Billen P., Leccisi E., Khalifa S., Spatari S., Fafarman A., Fthenakis V., Benefits and risks of lead halide perovskite photovoltaics, PV Magazine, Nov. 14, 2019 https://www.pv-magazine.com/2019/11/14/benefits-and-risks-of-lead-halide-perovskite-photovoltaics/ [43]

In this Opinion & Analysis article, we highlight the findings of our study of the life-cycle lead emissions and toxicity potential of LHP-PVs in comparison to US grid electricity mixes. We found that the lead emissions and toxicity potential associated with LHP-PVs are less than those associated with grid electricity, but we caution that proper industrial hygiene during manufacturing, robust encapsulation for durable operation, and end-of-life management are critical for responsible deployment of this technology.

- Leccisi E. and V. Fthenakis V., Life-cycle energy demand and carbon emissions of industrial production of single-junction and tandem perovskite PV, submitted to Energy and Environmental Science, October 10, 2020.

This article addresses challenges for perovskite solar cell (PSC) fabrication transitioning from laboratory to sustainable industrial production levels, and presents the development of life-cycle inventory (LCI) material and energy data for scalable production and comprehensive life-cycle-analyses (LCAs) and Net Energy Analysis (NEA) of most promising single-junction and tandem PSC systems. LCAs were conducted for four single- junction and three tandem devices with assumptions regarding scalable production validated by industry experts. It is shown that solution-based PSC manufacturing (i.e., spray coating and gravure printing) would be less impactful to the environment than devices fabricated with vapor-based methods, and that gravure roll-to-roll (RtR) printing of PSC offers the lowest life-cycle cumulative energy demand and carbon emissions among the considered material deposition processes. Contribution analysis of the impacts of each layer and material of perovskite devices shows, for example, that MoOx/Al is less impactful than Ag, and fluorine-tin-oxide (FTO) less impactful than indium-tin-oxide (ITO). The NEA estimated Energy Payback Times

(EPBT) and Energy Return on Energy Investment (EROI) of perovskite PV (PPV) systems are compared with those of the current production of commercial silicon and thin-film photovoltaics, assuming life expectancies of PPV between 10 and 30 years and new, up-to-date LCI data on silicon PV production. It is shown that PPV produced with RtR manufacturing could reach the same EROI as that of single-crystalline-Si PV within 12 years of life, whereas the most energy demanding PSC production with spray coating on rigid substrates, would require a 15-yr life to match the EROI of 30-yr lasting silicon PV. Comparisons with CdTe and CIGS thin-film PV are also reported.

9. Budget and Schedule:

The total project budget was $251,950 comprising $199,911 from DOE and $52,039 cost-share (20.61%) from Columbia U. However, during the project our cost-share resulted to $61,363, while the DOE funding remained the same; thus our final cost-share was 23.5% (details are shown in RPPR2).

The project started on March 1, 2019 and ended on July 31, 2020. However, we have been continuing work on publishing the project results at no-cost to DOE; we submitted a journal manuscript on October 10, 2020 and we are working on another manuscript that we plan to submit within the calendar year.

10. Path Forward:

Further research is needed on material management (cell/module materials and solvents) in emerging perovskite manufacturing, including recycling and industrial hygiene. Dr. Fthenakis and his team at Columbia U. (formerly at BNL) have unique expertise on investigating environmental health and safety issues in emerging PV technologies. Future DOE funding on this area would leverage such capability.

11. Inventions, Patents, Publications, and Other Results:

- E. Leccisi E. and V. Fthenakis, Critical Review of Perovskite LCA, *Progress in Energy*, 3(2) Published 24 July 2020, https://iopscience.iop.org/journal/2516-1083. [41]
- E. Leccisi and V. Fthenakis, Critical Review of Perovskite Photovoltaic Life Cycle Environmental Impact Studies, *2019 IEEE 46th Photovoltaic Specialists Conference (PVSC)*, Chicago, IL, USA, 2019, pp. 1-6, doi: 10.1109/PVSC40753.2019.9198977. [42]
- B. Baxter, P. Billen, E. Leccisi, S. Khalifa, S. Spatari, A. Fafarman, V. Fthenakis, Benefits and risks of lead halide perovskite photovoltaics*, PV Magazine*, Nov. 14, 2019 https://www.pv-magazine.com/2019/11/14/benefits-and-risks-of-lead-halide-perovskite-photovoltaics/. [43]
- E. Leccisi and V. Fthenakis, Life-cycle energy demand and carbon emissions of industrial production of single-junction and tandem perovskite PV, submitted to Energy and Environmental Science, October 10, 2020.

12. References:

1. Li, Z., Klein, T.R., Kim, D.H., Yang, M., Berry, J.J., van Hest, M.F. and Zhu, K., 2018. Scalable fabrication of perovskite solar cells. Nature Reviews Materials, 3(4), pp.1-20.
2. Espinosa, N., Serrano-Luján, L., Urbina, A. and Krebs, F.C., 2015. Solution and vapour deposited lead perovskite solar cells: Ecotoxicity from a life cycle assessment perspective. Solar Energy Materials and Solar Cells, 137, pp.303-310.
3. Serrano-Lujan, L., Espinosa, N., Larsen-Olsen, T.T., Abad, J., Urbina, A. and Krebs, F.C., 2015. Tin-and lead-based perovskite solar cells under scrutiny: an environmental perspective. Advanced Energy Materials, 5(20), p.1501119.
4. Gong, J., Darling, S.B. and You, F., 2015. Perovskite photovoltaics: life-cycle assessment of energy and environmental impacts. Energy & Environmental Science, 8(7), pp.1953-1968
5. Celik, I., Phillips, A.B., Song, Z., Yan, Y., Ellingson, R.J., Heben, M.J. and Apul, D., 2017. Environmental analysis of perovskites and other relevant solar cell technologies in a tandem configuration. Energy & Environmental Science, 10(9), pp.1874-1884.
6. Monteiro Lunardi, M., Wing Yi Ho-Baillie, A., Alvarez-Gaitan, J.P., Moore, S. and Corkish, R., 2017. A life cycle assessment of perovskite/silicon tandem solar cells. Progress in photovoltaics: research and applications, 25(8), pp.679-695.
7. Alberola-Borràs, J.A., Baker, J.A., De Rossi, F., Vidal, R., Beynon, D., Hooper, K.E., Watson, T.M. and Mora-Seró, I., 2018. Perovskite photovoltaic modules: life cycle assessment of pre-industrial production process. iScience, 9, pp.542-551.
8. Ibn-Mohammed, T., Koh, S.C.L., Reaney, I.M., Acquaye, A., Schileo, G., Mustapha, K.B. and Greenough, R., 2017. Perovskite solar cells: An integrated hybrid lifecycle assessment and review in comparison with other photovoltaic technologies. Renewable and Sustainable Energy Reviews, 80, pp.1321-1344.
9. Zhang, J., Gao, X., Deng, Y., Zha, Y. and Yuan, C., 2017. Comparison of life cycle environmental impacts of different perovskite solar cell systems. Solar Energy Materials and Solar Cells, 166, pp.9-17.
10. Alberola-Borràs, J.A., Vidal, R., Juárez-Pérez, E.J., Mas-Marzá, E., Guerrero, A. and Mora-Seró, I., 2018. Relative impacts of methylammonium lead triiodide perovskite solar cells based on life cycle assessment. *Solar Energy Materials and Solar Cells*, *179*, pp.169-177.
11. Sánchez, S., Vallés-Pelarda, M., Alberola-Borràs, J.A., Vidal, R., Jerónimo-Rendón, J.J., Saliba, M., Boix, P.P. and Mora-Seró, I., 2019. Flash infrared annealing as a cost-effective and low environmental impact processing method for planar perovskite solar cells. Materials Today, 31, pp.39-46.
12. Zhang, J., Gao, X., Deng, Y., Li, B. and Yuan, C., 2015. Life cycle assessment of titania perovskite solar cell technology for sustainable design and manufacturing. ChemSusChem, 8(22), pp.3882-3891.
13. Guinee, J.B., Heijungs, R., Huppes, G., Zamagni, A., Masoni, P., Buonamici, R., Ekvall, T. and Rydberg, T., 2011. Life cycle assessment: past, present, and future

14. Consoli, F. ed., 1993. Guidelines for Life-cycle Assessment: a'Code of Practice': From the SETAC Workshop Held at Sesimbra, Portugal, 31 March-3 April 1993. Society of Environmental Toxicology and Chemistry.
15. International Organization for Standardization, Standard ISO, 14040 Environmental Management – Life Cycle Assessment – Principles and Framework, 2006, https://www.iso.org/standard/37456.html, accessed September 2020.
16. International Organization for Standardization, Standard ISO, 14044 Environmental Management – Life Cycle Assessment – Requirements and guidelines, https://www.iso.org/standard/38498.htmla, accessed September 2020.
17. Fthenakis, V., Frischknecht, R., Raugei, M., Kim, H.C., Alsema, E., Held, M. and de Wild-Scholten, M., 2011, Methodology Guidelines on Life Cycle Assessment of Photovoltaic Electricity, 2nd edition, *Int Energy Agency PVPS Task 12*, 2011, Report IEA-PVPS T12-03:2011.
18. Frischknecht, R., Heath, G., Raugei, M., Sinha, P. and de Wild-Scholten, M., 2016. Methodology Guidelines on Life Cycle Assessment of Photovoltaic Electricity, 3rd edition, *Int. Energy Agency PVPS Task 12*, 2016, Report IEA-PVPS T12-06:2016.
19. Celik, I., Song, Z., Cimaroli, A.J., Yan, Y., Heben, M.J. and Apul, D., 2016. Life Cycle Assessment (LCA) of perovskite PV cells projected from lab to fab. Solar Energy Materials and Solar Cells, 156, pp.157-169.
20. Itten, R. and Stucki, M., 2017. Highly efficient 3rd generation multi-junction solar cells using silicon heterojunction and perovskite tandem: prospective life cycle environmental impacts. Energies, 10(7), p.841.
21. Billen, P., Leccisi, E., Dastidar, S., Li, S., Lobaton, L., Spatari, S., Fafarman, A.T., Fthenakis, V.M. and Baxter, J.B., 2019. Comparative evaluation of lead emissions and toxicity potential in the life cycle of lead halide perovskite photovoltaics. Energy, 166, pp.1089-1096.
22. Alberola-Borràs, J.A., Vidal, R. and Mora-Seró, I., 2018. Evaluation of multiple cation/anion perovskite solar cells through life cycle assessment. Sustainable Energy & Fuels, 2(7), pp.1600-1609.
23. García-Valverde, R., 2010. J. a. Cherni and A. Urbina. Prog. Photovoltaics Res. Appl, 18, pp.535-538.
24. M. McGehee, Progress on Gen. V Perovskite-Si Tandems. PVRD2 8167 Q3 Report, 2019.
25. A. Palmstrom, G. Eperon, T. Leijtens, R. Prasanna, S. Habisreutinger, W. Nemeth, A. Gaulding, S. Dunfield, R. Matthew, S. Nanayakkara, T. Moot, J. Werner, J. Liu, T. Bobby, S. Christensen, M. McGehee, M. van Hest, J. Luther, J. Berry and D. Moore D, Joule, 2019, 3, 2193-2204.
26. Fraunhofer Institute for Solar Energy Systems, Photovoltaics Report, 2020, https://www.ise.fraunhofer.de/content/dam/ise/de/documents/publications/studies/Photovoltaics-Report.pdf, accessed September 2020.
27. National Renewable Energy Laboratory (NREL), Best Research-Cell Efficiency Chart, 2020, https://www.nrel.gov/pv/cell-efficiency.html, accessed September 2020.

28. Raugei, M., Sgouridis, S., Murphy, D., Fthenakis, V., Frischknecht, R., Breyer, C., Bardi, U., Barnhart, C., Buckley, A., Carbajales-Dale, M. and Csala, D., 2017. Energy Return on Energy Invested (ERoEI) for photovoltaic solar systems in regions of moderate insolation: A comprehensive response. Energy Policy, 102, pp.377-384.
29. Carbajales-Dale, M., Barnhart, C.J., Brandt, A.R. and Benson, S.M., 2014. A better currency for investing in a sustainable future. Nature Climate Change, 4(7), pp.524-527.
30. Raugei, M., 2019. Net energy analysis must not compare apples and oranges. Nature Energy, 4(2), pp.86-88.
31. Hall, C., Lavine, M. and Sloane, J., 1979. Efficiency of energy delivery systems: I. An economic and energy analysis. Environmental Management, 3(6), pp.493-504.
32. Raugei, M., Frischknecht, R., Olson, C., Sinha, P. and Heath, G., 2016. Methodological guidelines on net energy analysis of photovoltaic electricity, *International Energy Agency PVPS,* 2016, IEA Report T12- 07:2016.
33. Leccisi, E., Raugei, M. and Fthenakis, V., 2016. The energy and environmental performance of ground-mounted photovoltaic systems—a timely update. Energies, 9(8), p.622.
34. Raugei, M., Peluso, A., Leccisi, E. and Fthenakis, V., 2020. Life-Cycle Carbon Emissions and Energy Return on Investment for 80% Domestic Renewable Electricity with Battery Storage in California (USA). Energies, 13(15), p.3934.
35. International Technology Roadmap for Photovoltaic ITRPV 2020, https://itrpv.vdma.org, accessed September 2020.
36. Frischknecht, R., Itten, R., Sinha, P., de Wild-Scholten, M., Zhang, J., Heath, G.A. and Olson, C., 2015. Life Cycle Inventories and Life Cycle Assessment of Photovoltaic Systems, International Energy Agency, *Int. Energy Agency Photovoltaic PVPS Task 12*, 2015, Report T12-04:2015.
37. Espinosa, N., Garcia-Valverde, R., Urbina, A. and Krebs, F.C., 2011. A life cycle analysis of polymer solar cell modules prepared using roll-to-roll methods under ambient conditions. Solar Energy Materials and Solar Cells, 95(5), pp.1293-1302.
38. CML-IA Characterisation Factors, Universiteit Leiden, 2016 http://www.universiteitleiden.nl/en/research/research-output/science/cml-ia-characterisation-factors, accessed September 2020.
39. Rosenbaum, R.K., Bachmann, T.M., Gold, L.S., Huijbregts, M.A., Jolliet, O., Juraske, R., Koehler, A., Larsen, H.F., MacLeod, M., Margni, M. and McKone, T.E., 2008. USEtox—the UNEP-SETAC toxicity model: recommended characterisation factors for human toxicity and freshwater ecotoxicity in life cycle impact assessment. The International Journal of Life Cycle Assessment, 13(7), p.532.
40. USEtox, https://usetox.org, accessed on September 2020.
41. Leccisi, E. and Fthenakis, V., 2020. Life-cycle environmental impacts of single-junction and tandem perovskite PVs: A critical review and future perspectives. *Progress in Energy 2,* 032002, https://doi.org/10.1088/2516-1083/ab7e84.

42. Leccisi E. and Fthenakis V., Critical Review of Perovskite Photovoltaic Life Cycle Environmental Impact Studies, *2019 IEEE 46th Photovoltaic Specialists Conference (PVSC)*, Chicago, IL, USA, 2019, pp. 1-6, doi: 10.1109/PVSC40753.2019.9198977.
43. Baxter J., Billen P., Leccisi E., Khalifa S., Spatari S., Fafarman A., Fthenakis V., Benefits and risks of lead halide perovskite photovoltaics, PV Magazine, Nov. 14, 2019 https://www.pv-magazine.com/2019/11/14/benefits-and-risks-of-lead-halide-perovskite-photovoltaics/.